

An Optimistic-Robust Approach for Dynamic Positioning of Omnichannel Inventories

Pavithra Harsha, Shivaram Subramanian, Ali Koc, Mahesh Ramakrishna, Brian Quanz, Dhruv Shah, Chandra Narayanaswami
 IBM T. J Watson Research Center, Yorktown Heights, NY 10570s
 Author Contact: pharsha@us.ibm.com

We introduce a new class of data-driven and distribution-free optimistic-robust *bimodal* inventory optimization (BIO) strategy to effectively allocate inventory across a retail chain to meet time-varying, uncertain omnichannel demand. The bimodal nature of BIO stems from its ability to balance downside risk, as in traditional Robust Optimization (RO), which focuses on worst-case adversarial demand, with upside potential to enhance average-case performance. This enables BIO to remain as resilient as RO while capturing benefits that would otherwise be lost due to endogenous outliers. Omnichannel inventory planning provides a suitable problem setting for analyzing the effectiveness of BIO’s bimodal strategy in managing the tradeoff between lost sales at stores and cross-channel e-commerce fulfillment costs, factors that are inherently asymmetric due to channel-specific behaviors. We provide structural insights about the BIO solution and how it can be tuned to achieve a preferred tradeoff between robustness and the average-case performance. Using a real-world dataset from a large American omnichannel retail chain, a business value assessment during a peak period indicates that BIO outperforms pure RO by 27% in terms of realized average profitability and surpasses other competitive baselines under imperfect distributional information by over 10%. This demonstrates that BIO provides a novel, data-driven, and distribution-free alternative to traditional RO that achieves strong average performance while carefully balancing robustness.

Key words: Bi-modal strategy, ally-adversary, Kelly’s criterion, omnichannel, two-stage robust optimization, inventory management, uncertainty, applications

History:

1. Introduction

An increasingly digital economy has led to a proliferation of virtual shopping channels, making omnichannel shopping ubiquitous among today’s consumers, a trend that extends across diverse product categories as well as emerging markets that were previously dominated by brick-and-

mortar retailing (NeilsonIQ 2022). The immediacy of this omnichannel consumer demand has driven today’s supply chains to be agile and responsive. For example, retail chains now offer various delivery options in addition to serving walk-in customers. These options often come with service guarantees, such as same-day delivery, free two-day shipping, and buy-online-pick-up-in-store (BOPUS) within two hours. To serve this diversified consumer demand, retailers have opened multiple facilities to minimize fulfillment costs and expedite delivery. They also employ cross-fulfillment methods such as serving demand from distant warehouses or utilize ship-from-store (SFS) to reduce lost sales opportunities and/or meet on-time delivery targets.

The dynamics in the retail industry in 2020 due to the pandemic have forced retailers to think much more broadly and invest more rapidly in their omnichannel capabilities (Bourlier 2020). In fact, the digital transformation is prompting companies to also pool their omnichannel capabilities, including physical assets like warehouse space or last-mile transportation, as well as information, leading to mutual profitability and propelling them further ahead in their omnichannel journey (Saéñz et al. 2022).

Omnichannel inventory systems (OIS) are an essential component of this rapid shift from product-centric to customer-centric supply chains. Optimal inventory positioning across the retail chain is a critical aspect of OIS and aims to place the right amount of inventory in the right location to serve omnichannel demand. The traditional planning methods that are siloed by channel and/or location fall short of this goal due to conflicting assumptions on how the inventory is used for downstream fulfillment. This may lead to stock-outs, particularly among walk-in and BOPUS customers, low margins due to expensive fulfillment costs for online demand, excessive carrying costs, and price markdowns. To mitigate these challenges, network-based planning models that incorporate fulfillment flexibility of the e-commerce demand (and simultaneously the inflexibility in meeting walk-in demand) are key to tap into the efficiencies of cross-channel and cross-location resource pooling.

Our work aims to develop a data-driven distribution-free network-based inventory management policy for the OIS that optimizes the quantity of inventory that is periodically purchased and

positioned in the retail chain to dynamically match the supply with time-varying and uncertain omnichannel demands to maximize the retail chain's total profit margins with the dual goals of maximizing sales and minimizing fulfillment costs.

Robust inventory planning, which is inherently data-driven and distribution free, primarily focuses on the *downside* objective, i.e., worst-case demand scenarios and mitigating risks associated with adversarial demand patterns. However, to be truly customer-centric, an OIS must equally be able to take advantage of the *upside* of making inventory positioning decisions that drive long-term profitable sales and grow its customer base. Achieving both resilience against negative outcomes and the ability to seize positive opportunities requires a *bimodal* resource allocation strategy—one that not only safeguards against worst-case demand but also optimizes for potential gains. This dual approach, which retains data-driven and distribution-free properties, has received less attention in the robust optimization (RO) literature and is the focus of this paper. We argue that a bimodal inventory management strategy is particularly valuable for balancing the tradeoff between lost sales at physical stores and the costs of cross-channel e-commerce fulfillment, which is at the core of our model. These tradeoffs are asymmetric due to the heterogeneous behavior of different channels, with store inventory facing higher lost sales costs, while e-commerce fulfillment depends on network effects. Hence, omnichannel inventory planning is a challenging problem setting for analyzing the effectiveness of BIO's bimodal strategy. The contributions of this paper are as follows:

1. We propose a optimistic-robust replenishment policy based on a data-driven, distribution-free Bimodal inventory optimization (BIO) model that optimizes the allocations using a convex combination of best- and worst-case demand scenarios via an user-chosen optimism hyperparameter. Pure adversarial models seek to misalign demands from inventory resulting in sales that are less responsive to increased (but potentially skewed) inventory allocations resulting in overly pessimistic replenishment decisions. BIO models overcome this limitation, specifically the presence of decision-dependent outliers, by simultaneously balancing the best- and worst-case scenarios.

2. We provide insights into the structure of the optimal allocation of the BIO problem by showing that under the optimal allocation follows the same blending of the best- and worst- case optima

as the user-selected scenario blending. This establishes a relatively easy mechanism to identify the corresponding optimal allocation via a simple out-of-sample evaluation, enabling decision-makers to determine an allocation that achieves a desired balance between objectives, such as expected profit and robustness.

3. Next, we derive an exact linear reformulation of the adversarial bi-linear BIO sub-problem. This is achieved by demonstrating and leveraging the integrality of the extreme points within the selected uncertainty set, which is constructed using inputs from a demand forecasting model. The derived sub-problem is then employed within a column and cut generation (CCG) algorithm. This algorithm is utilized to solve large-scale real-world BIO instances characterized by generalized fulfillment cost structures, operational restrictions, and omnichannel business constraints.

4. Last, we perform extensive Monte Carlo simulation experiments using real data of a retail chain that operates over 150 stores spread across the continental United States. We observe that the incremental benefit of BIO models, including pure RO, is pronounced in the context of omnichannel operations over the baseline models (which are otherwise optimal in a pure walk-in setting). This advantage arises from the effective utilization of cross-channel resource pooling. We observe that the BIO models can enhance the performance of the pure RO models on average by up to 10% by tuning a single optimism hyper-parameter across different parameter and initial inventory settings. In a comprehensive business value assessment over a rolling horizon with a realistic fine-grained customer transaction level fulfillment engine, we observe that BIO outperforms pure RO by 27% in terms of realized average profitability and surpasses other competitive baselines under imperfect distributional information by over 10%. This demonstrates that BIO provides a novel, data-driven, and distribution-free alternative to traditional RO that achieves strong average performance while carefully balancing robustness.

We would like to note that our modeling choices address several practical considerations including: (1) very low-rate of sales interspersed with brief but sharp sales peaks where the shared inventory system is stretched to capacity, (2) the degree of uncertainty in multi-period, multi-channel

demand forecast are inputs generated by AI/ML models, (3) the cascading effects of decisions span across a large omnichannel network consisting of hundreds of nodes, (4) the manifold impact of lead times, cross-fulfillment costs, and lost sales opportunities, and finally (5) to demonstrate practical effectiveness on real-world data in a multi-period rolling horizon setting.

2. Related Literature

We classify the related literature into three main areas: (1) Inventory management considering cross-fulfillment, transshipment, and omnichannel retailing; (2) RO, distributional, and Pareto robust techniques; and (3) Kelly's principle.

Inventory management with cross-fulfillment considerations is a topic of growing interest in the operations management community. The pioneering paper of Acimovic and Graves (2017) studies the periodic-review joint-replenishment problem for a group of fulfillment centers (FCs) serving e-commerce demand. They propose heuristic policies to mitigate costly demand spill overs across FCs assuming a myopic fulfillment policy in the presence of lead times. This paper and those we describe next advocate the need for integrated planning across locations rather than decentralized strategies, when cross-fulfillment is involved. Bandi et al. (2019) develop robust-periodic affine policies for newsvendor networks in a backorder setting for single and multiple items. Lim et al. (2021) presents a two-phase RO approach (binary decision variables in phase 1 with an elastic uncertainty set and continuous decision variables in phase 2) to the joint replenishment and fulfillment problem for e-commerce networks with drop shipment (no backlog or lost sales). Govindarajan et al. (2021a) develop a semi-definite programming (SDP) based heuristic to solve the distributionally robust multi-location inventory allocation problem on a newsvendor network (single period, e-commerce channel) assuming a L-level nested fulfillment cost structure. These single channel e-commerce models as well as the traditional pure walk-in channel models (see Jackson et al. 2019 and the references therein), cannot be used for omnichannel setting precisely because we have to simultaneously account for the inability to cross-fulfill store demand and the flexibility to do so for online demand across multiple locations.

Govindarajan et al. (2021b) develop a heuristic for the joint initial positioning and fulfillment of a seasonal item in a lost sales omnichannel setting. They require distributional assumptions at all locations and assume that (1) any unfulfilled store demand can be cross-fulfilled and (2) the fulfillment cost has an L-level nested structure. Our paper also focuses on the multi-location omnichannel setting with lost sales, but considers the problem of periodic replenishment with lead times and general fulfillment cost structures, without relying on the aforementioned assumptions. We explicitly consider the tradeoff between the lost walk-in sales at stores and cross-channel fulfillment costs that prior single channel or omnichannel models do not address.

The reactive nature of fulfillment is analogous to a zero-transshipment setting with no lead time (Yang and Qin 2007). For an extensive review of this topic, readers can refer to Paterson et al. (2011). Transshipment problems, in general, are intractable (Tagaras and Cohen 1992), and by extension, it is the case with the replenishment problem with fulfillment that we study.

Omnichannel retailing more broadly (and encompassing inventory management) has received increasing attention in the literature with several works analyzing the impact of inventory and product information sharing across channels (Gallino and Moreno 2014, Gao and Su 2017b), fulfillment optimization (Acimovic and Graves 2015, Jasin and Sinha 2015, Ali et al. 2017), fulfillment flexibility (DeValve et al. 2023), omnichannel pricing (Lei et al. 2018, Harsha et al. 2019a,b), and store pick-ups (Gallino et al. 2017, Gao and Su 2017a) and returns (Nageswaran et al. 2020).

Robust Optimization (RO) is a widespread methodology for modeling decision-making problems under uncertainty and it seeks to optimize the worst-case performance across all scenarios within the pre-specified uncertainty set (see Bertsimas et al. 2011, Gorissen et al. 2015, and the robust inventory management papers referenced above and the references there-in). A long standing criticism of RO, especially among practitioners is that it produces overly conservative decisions. Iancu and Trichakis (2014) propose models that can identify pareto-optimal robust (PRO) solutions that perform just as well in the worst case and same or better in non-worst case scenarios. One well-studied approach to identify practical viable solutions is to use budget constraints that are derived

from limit laws to contain the variability (Bandi and Bertsimas 2012). A limitation of this approach we observe in our setting is the inability of RO to overcome endogenous outliers that continues to result in conservative solutions (for e.g., those that can only be eliminated by decision dependent limit-based uncertainty sets whose budget bounds are hard to characterize in closed form, see Section 4 for a motivating example). Another recent work motivates variable (box) uncertainty sets that can be tuned in accordance with user-specified cost target (Lim and Wang 2017). In this paper, we derive data-driven hierarchical budget constraints (in similar spirit to the limit laws) as an independent, fixed input from a demand forecasting model.

Distributionally robust optimization (DRO) is yet another paradigm to mitigate conservatism by seeking to identify the worst-performing distribution from an ambiguity class (Rahimian and Mehrotra 2019). Recently Gotoh et al. (2023) introduce a class of distributionally optimistic optimization (DOO) models and show that it is always possible to outperform the (finite sample) SAA if ones considers both worst- and best-case methods, noting that the optimistic solutions more sensitive to model error than either worst-case or SAA optimizers. In contrast to the pure worst-case (RO, DRO) or pure best-case (DOO), the bi-modal inventory management strategy BIO that we introduce leverages an allied-adversary that simultaneously seeks to gain from potential upsides while managing an adversary across scenarios within a given uncertainty set.

Our approach is inspired by the seminal work of Kelly (1956) that examines the problem of maximizing the growth rate of wealth over a series of independent trials to identify an optimal fraction of resources to bet under uncertainty assuming re-investment. The optimal ‘Kelly criterion’ for this specific problem setting is an analytically derived value that lies between the twin extremes of maximizing expected gain (invest as much as possible) and minimizing the probability of ruin (invest as little as possible) in order to achieve long-term gain (Rotando and Thorp 1992). We see a parallel to Kelly’s bimodal decision-making approach within our multi-period robust inventory optimization problem where we seek a balance between procuring and positioning significant inventory levels spread uniformly across the network versus procuring optimistically low quantities and positioning them in alignment with confident point forecasts. However, unlike Kelly’s framework, our setting does not involve periodic reinvestment and the resulting compounding gains or losses.

3. Problem setting, notation and assumptions

Consider an omnichannel retailer selling a single item and operating a network of retail stores and warehouses, both of which we refer to as nodes and denote by Λ . The retailer serves walk-in demand and e-commerce demand and uses the inventory in the stores and warehouses to fulfill the demands in various channels, in particular, the store inventory to meet its walk-in demand and the network inventory across nodes for online demand. The goal of the retailer is to purchase inventory from a supplier S and distribute this across the different nodes in the network to maximize profitability over a finite forward looking time horizon \mathcal{T} , assuming that any unmet demand is lost. In Appendix A, we provide the modifications to the models if we additionally consider re-positioning of inventory between different nodes of the network. We explain the key variables, the parameters, the sequential decision programming framework and our assumptions next, while the detailed notations are described in Table 3.

State: The state denoted by \mathbf{I} comprises of the current on-hand inventory and that in the pipeline for all $l \in \Lambda$. At time t for location l , the state is I_{tl}^j where $j = 0, \dots, L_l$ where L_l is the deterministic lead time to node l with index 0 referring to on-hand inventory. The initial inventory is $\bar{\mathbf{I}}$.

Action: The retailer aims to make a decision x_{tl} for all $l \in \Lambda$ which is the quantity of inventory to purchase and move from the supplier node S to node l at time t . Although we model and solve for decisions across all the \mathcal{T} periods, we only execute on the current decisions, i.e., decisions are made in a rolling horizon fashion. In practice, the demand forecast is periodically updated based on realized demands and the optimization model is re-solved. A multi-period problem is essential to account for the positive lead time, specifically the future impact of decisions taken in the current period and avoid trivial myopic solutions.

Uncertainty: We model the walk-in demand at the node level and the e-commerce demand at a region level that we refer to as zones Z . A zone is a geographically contiguous cluster of zip-codes that have the same cost of shipping from any given origin node. We denote the uncertain walk-in and online demands at node $l \in \Lambda$ and zone $z \in Z$ by D_{tl}^b and D_{tz}^o respectively.

Table 1 Notation for the model.

Indices and Sets	
$l, z, t,$	a node (store or warehouses), a zone, a period,
$o, b,$	the online channel, the brick-and-mortar channel,
$\Lambda, Z,$	all nodes, all zones,
$\mathcal{T},$	all time periods $\{0 \dots T - 1\}$ where T is the planning horizon,
$S,$	supplier node,
Parameters	
$p_{il}^b, b_{il}^b,$	price, lost sales penalty for store l sales in period $t,$
$p_t^o, b_t^o,$	price, lost sales penalty for online sales in period $t,$
$h_l,$	holding cost at node l of left over inventory in a period,
c_{lz}	unit cost of fulfilling an online order in zone z from node $l,$
$C_l,$	unit purchase & transportation cost from supplier S to node $l,$
$L_l,$	lead time between supplier node S to node $l,$
$\bar{I}_l^j,$	initial inventory pipeline for node l arriving in j periods,
Decision Variables	
$I_{il}^j,$	inventory for node l in period t arriving in j periods,
$x_{it},$	inventory allocated from supplier in period t for node $l,$
$s_{il}^b,$	fulfilled, lost demand from store l in period $t,$
$s_{tz}^{oS},$	fulfilled, lost online demand from zone z in period $t,$
$y_{iltz},$	fulfilled online demand in zone z from node l in period $t.$

Reward: To compute the retailer's profitability, we are given (non-negative) prices and back-order penalties in the different channels in the down stream periods. They are denoted by p_{il}^b, b_{il}^b for walk-in demand and p_t^o, b_t^o for online demand. Note that the walk-in prices and penalties can vary by location while e-com prices are fixed across locations. We assume that $p_{il}^b + b_{il}^b > p_t^o + b_t^o - c_{lz} \forall i \in \Lambda, z \in Z, t \in \mathcal{T}$ where c_{lz} is the fulfillment cost from node l to any zone z . This assumption effectively enforces a service priority for a walk-in customer over an online order, thus avoiding stock hedging (hiding inventory in the backroom) for an potential online customer rather than serving an existing walk-in customer. We also assume that prices and penalties are non-increasing over time to avoid a similar stock hedging phenomenon over time and ensure that it is preferable to fulfill an existing order now rather than wait until a future time period. Let h_l denote the holding cost for left over inventory in node l in any period and C_l denote the combined purchase and transportation cost of moving inventory from the supplier to node l .

Sequence of events: The inventory in the pipeline arrives and the retailer places an order with the supplier. For nodes with zero lead time, the order arrives immediately. Then, the omnichannel demand realizes, after which the retailer fulfills it. Finally, the rewards and costs are incurred.

Fulfillment assumptions: Note that for the purpose of making inventory purchase and distribution decisions, we assume that the fulfillment decisions are batched within each period. In practice, fulfillment is realized exogenously (to the model) based on customer arrivals and handled by the

retailer’s order management system (OMS). This is an independent system that determines the fulfilling store or warehouses on-the-fly for e-commerce customer orders based on a variety of metrics including operational costs, capacity balancing across nodes, stock outs, markdowns and can also involve complex and dynamic rules that depend on store performance, traffic, and capacity, local weather, and order splitting rules, among other factors (Ali et al. 2017). Unlike fulfilment, inventory decisions follow a more regular cadence (say bi-weekly or weekly) and are usually dependent on the transportation schedule of trucks.

Optimization paradigm: To optimize the expected cost using stochastic programming, the future demand uncertainty has to be characterized via high dimensional probabilistic models and/or via complex scenarios generation techniques that characterize the dependence across the random variables. Due to its challenging nature and the dependence of the solution on inexact estimations of the true distribution that can adversely affect real-life performance, we adopt a framework that builds on the data-driven robust optimization (RO) paradigm.

Uncertainty set: In the RO paradigm, the retailer aims to maximize the worst case total profitability assuming the demand, D_{tl}^b and D_{tz}^o , are uncertain and comes from a pre-specified polyhedral set U derived from data. Specifically, we assume the following structure for U :

$$U := \left\{ \mathbf{D}_t^b, \mathbf{D}_t^o \forall t \in \mathcal{T} \left| \begin{array}{ll} \bar{\mathbf{D}}_t^{mL} \leq \mathbf{D}_t^m \leq \bar{\mathbf{D}}_t^{mU} & \forall m \in \{o, b\}, t \in \mathcal{T} \\ \bar{\bar{\mathbf{D}}}_t^{mL} \leq \mathbf{e}^T \mathbf{D}_t^m \leq \bar{\bar{\mathbf{D}}}_t^{mU} & \forall m \in \{o, b\}, t \in \mathcal{T} \end{array} \right. \right\}, \quad (3.1)$$

Here \mathbf{e} refers to a vector of 1 and \mathbf{D}_t^m refers to the vector of demand across locations (nodes or zones depending on channel m). The first constraint in (3.1) restricts the channel-location-period specific demand to a box set and the second, referred to as the budget constraint, requires the channel-period specific total demand across locations to fall within a lower and an upper bound. The budget bounds are derived through quantile modeling of demand distributions at both local and hierarchical levels in a data-driven manner. For example, this can be achieved by learning from historical demand data using quantile-based models—an entirely data-driven approach. In our experiments with real-data, we developed channel specific multi-task demand models across

locations (or zones for e-commerce) with a focus on accuracy and coherency across the location hierarchy. Multi-task models learn shared/common effects (correlations) across different time-series by utilizing common features (Salinas et al. 2019, Oreshkin et al. 2020, Makridakis et al. 2022, Jati et al. 2023).

In the absence of a hierarchical forecast, one can fall back on central-limit theorem based location-scale normalized budget constraints (Bertsimas and Sim 2004, Bandi and Bertsimas 2012). Unlike a hierarchical forecast, the location-scale method requires a variance estimator at the local level. Regardless of the nature of explicit (former) or implicit (latter) pooling methods discussed, budget constraints allow the decision maker to be less conservative and focus on the most probable set of scenarios. Additional cross-channel and/or multi-period budget constraints can also be included in practice. We work with a simple (effective and data-driven) uncertainty set for ease of exposition, and simple modifications suffice to incorporate alternative choices of budget-constrained sets.

4. Omnichannel robust inventory optimization model

The adaptive multi-period RO model can now be formulated as follows:

$$Z_R^*(\bar{\mathbf{I}}) = \max_{\mathbf{x}_t(\mathbf{D}[0:t-1]) \geq 0} \min_{\mathbf{D}[0,T] \in U} \max_{\substack{\{\mathbf{s}_t, \mathbf{y}_t, \mathbf{I}_{t+1}\} \in \\ F(\mathbf{I}_t, \mathbf{D}_t, \mathbf{x}_t(\mathbf{D}[0:t-1]))}} \sum_{t \in \mathcal{T}} O(\mathbf{s}_t, \mathbf{y}_t, \mathbf{I}_{t+1}, \mathbf{D}_t, \mathbf{x}_t(\mathbf{D}[0:t-1])) \quad (4.1)$$

$$\text{subject to.} \quad \mathbf{I}_{0l} = \bar{\mathbf{I}}_l \quad \forall l \in \Lambda \quad (4.2)$$

where the objective is:

$$\begin{aligned} O(\mathbf{s}_t, \mathbf{y}_t, \mathbf{I}_{t+1}, \mathbf{D}_t, \mathbf{x}_t) = & \sum_{l \in \Lambda} \left[p_{tl}^b s_{tl}^b - b_{tl}^b (D_{tl}^b - s_{tl}^b) \right] + \sum_{z \in Z} \left[\sum_{l \in \Lambda} (p_t^o - c_{tz}) y_{tlz} - b_t^o \left(D_{tz}^o - \sum_{l \in \Lambda} y_{tlz} \right) \right] \\ & - \sum_{l \in \Lambda} [h_l I_{t+1,l}^0 + C_l x_{tl}] \end{aligned} \quad (4.3)$$

and the fulfillment set $F(\mathbf{I}_t, \mathbf{D}_t, \mathbf{x}^t)$ is the set $\{\mathbf{s}_t, \mathbf{y}_t, \mathbf{I}_{t+1}\} \geq 0$ that satisfies the following constraints:

$$s_{tl}^b \leq D_{tl}^b \quad \forall l \in \Lambda, \quad (4.4)$$

$$\sum_{l \in \Lambda} y_{tlz} \leq D_{tz}^o \quad \forall z \in Z, \quad (4.5)$$

$$s_{tl}^b + \sum_{z \in Z} y_{tlz} + I_{t+1,l}^0 = I_{tl}^0 + I_{tl}^1 \mathbb{1}_{L_l > 0} + x_{tl} \mathbb{1}_{L_l = 0} \quad \forall l \in \Lambda, \quad (4.6)$$

$$I_{t+1,l}^j = I_{tl}^{j+1} \mathbb{1}_{j < L_l} + x_{tl} \mathbb{1}_{j = L_l} \quad \forall 1 \leq j \leq L_l, l \in \Lambda \quad (4.7)$$

This model is an adaptive multi-stage optimization problem with 3 stages in each period: inventory purchase and distribution, followed by the adversary choosing the worst-case demand, and finally, the retail fulfillment. Observe that the inventory decision variables x_{tl} are non-anticipatory and fully adjustable/adaptive (i.e., not static and depend on all prior realizations of demand $\mathbf{D}[0, t-1]$). The objective function (4.3) models the total profitability of the retailer from allocation, distribution and fulfillment. The first and second terms represents the profit from the store and e-commerce channels respectively and are obtained as the difference of the respective channel-specific revenue less the lost sales penalty cost. The third term sums the holding cost from the left over inventory, and the purchase cost from supplier and/or the transportation cost to move inventory from the supplier to the nodes. As far as the fulfillment constraint set, the constraints (4.4-4.5) ensures that the sales is less than the channel specific demand in every period and location. Constraint (4.6) enforces inventory balance for each location and time period. Finally, constraint (4.7) updates the state (i.e., the inventory pipeline).

The above formulation can be enhanced with business rules to capture retailer-specific operational requirements. For example, we can specify transportation capacities on x_{tl} and fulfillment capacities on y_{tlz} and create y_{tlz} variables only for edges lz originating from SFS eligible nodes. If the retailer prefers warehouse fulfillment of online demand to stores, the cost c_{lz} can be modified to reflect the additional savings, i.e., labor savings besides shipping cost. Some retailers set internal on-time delivery service targets, e.g., 80% of all e-commerce fulfillment should be delivered in 2 days. Such a goal can be implemented as follows: $\sum_{\{lz\} \in A} y_{tlz} \geq 0.8 \sum_{l \in \Lambda, z \in Z} y_{tlz}$ where $A = \{l \in \Lambda, z \in Z \mid \text{delivery time between } l \text{ and } z \text{ is less than 2 days}\}$. Such goals encourage the positioning of the inventory closer to the customer, an aspect that is important to consider in an omnichannel world. Today's customer has diverse delivery options including 2-hour delivery and curbside pickup, and demand can immediately turn into lost sales if the product is not available to a customer within the specified time-window.

For simplicity of exposition of the core *bimodal optimistic-robust* idea, we consider a static policy for the inventory decisions where the dependence of \mathbf{x}_t on demand $\mathbf{D}[0, t-1]$ is dropped, while

keeping the adaptive nature of fulfillment decisions intact. The problem here reduces to a two-stage NP-hard problem (Ben-Tal et al. 2004) that we solve via cut-generation techniques in Section 5. Note that the drawback of a static policy is its inability to adapt to new information in future periods, leading to myopic decisions. In contrast, while an adaptive policy is more responsive, it suffers from the curse of dimensionality when handling large state spaces. As mentioned in Section 3, decisions of the static policy are executed only for the current period, and the next static policy is recomputed in a rolling-horizon fashion, allowing for some adaptability. The optimistic-robust ideas proposed in this paper for static policies extend to alternative heuristic approaches, such as affine policies for adaptive decisions (see Ben-Tal et al. 2004).

4.1. Static robust policy to omnichannel inventory management

For concreteness, the formulation is as follows:

$$Z_{SR}^*(\bar{\mathbf{I}}) = \max_{\mathbf{x}_t \geq 0} \min_{\mathbf{D}_{[0,T]} \in U} \max_{\{\mathbf{s}_t, \mathbf{y}_t, \mathbf{I}_{t+1}\} \in F(\mathbf{I}_t, \mathbf{D}_t, \mathbf{x}_t)} \sum_{t \in \mathcal{T}} O(\mathbf{s}_t, \mathbf{y}_t, \mathbf{I}_{t+1}, \mathbf{D}_t, \mathbf{x}_t) \quad (4.8)$$

We simplify constraints (4.2), (4.6), and (4.7) by eliminating the inventory pipeline variables I_{tl}^j for all j by using the static inventory variables instead. Dropping the superscript j , we obtain:

$$s_{tl}^b + \sum_{z \in Z} y_{tlz} + I_{t+1,l} = I_{tl} + \bar{I}_l^{t+1} \mathbb{1}_{t < L_l} + x_{t-L_l,l} \mathbb{1}_{t \geq L_l} \quad \forall l \in \Lambda, \quad (4.9)$$

$$I_{0l} = \bar{I}_l^0 \quad \forall l \in \Lambda. \quad (4.10)$$

Insights into the solution structure: *Typical behavior of the static robust adversary (inner min-max problem) is to select skewed worst-case demands that do not align with inventory. This can be gathered by observing the objective terms in Eq. (4.3). Barring the last term (noting that x is fixed for the inner problem), each term results in a drop in profitability without a sale. Therefore, skewed inventory allocations x are of little value in the worst case as they result in no revenue and increased costs. So, a typical robust solution tends to be a fair and uniform distribution of inventory across locations so that the adversary does not benefit from a skewed choice of demand. This is a valuable feature of robust solutions in contrast to their deterministic counterparts. This result was proved in Govindarajan et al. (2021a) for a special case.*

Another aspect in the omnichannel environment is the *asymmetrical adversarial behavior that impacts the walk-in channel far more than the online channel*. Unlike walk-in demand, any online order can be satisfied using SFS fulfillment even when the inventory positioning is unfavorable.

Downsides of a robust solution: *Robust models are overly focused on protecting downside and ignore potential upside and tend to undervalue a wide-range of allocations*. Consider, for example, the robust model applied to 3 symmetric locations with just walk-in demand that satisfy a local budget of $[0,3]$ in each location and a global bound of $[1,6]$. The adversarial sales with no initial inventory at all locations does not increase even when one of the locations has high inventory, i.e., allocation $[0,0,0]$ has the same adversarial sales as allocation $[0,0,3]$ for example (with $[3,3,0]$ as the only adversarial sales in the latter and there are many more degenerate options including this for the former). In real-world data with several nodes, it is rare that the scenarios are so adversarial in nature that demand practically mis-aligns with inventory everywhere. On the contrary, with non-adversarial distributions *statistically there is a lower chance of lost sales in locations with higher inventory, which the robust model with its chosen objective and budget constraints fails to capture*. This results in endogenous outliers in the uncertainty set which are chosen as the optimal adversarial response. This outlier effect is magnified by the initial inventory variations across locations that increase the asymmetry and result in optimizing for adversarial scenarios that are rarely encountered.

We therefore propose an alternative RO approach that uses the idea of an ‘allied-adversary’ that incorporates the optimism associated with a increase sell-through that can occur with higher allocations. We continue to work within the RO framework for ease of model specification and to avoid the solution dependence on several uncertain probability estimates across the network.

4.2. Optimistic-robust optimization: An ally-adversary model

A high-level idea in Kelly’s approach that motivates our model is to view inventory purchase from a supplier and its positioning as a sequence of investment contributions to a portfolio of store locations. Here the decision maker not only positions herself for the adversarial worst case but

simultaneously explores profitable inventory purchase and positioning decisions that boost cumulative (expected) gain. Toward this goal, we extend the aforementioned distribution-free unimodal RO model and propose a distribution-free *bimodal* RO formulation that also analyzes the most favorable store demands that are aligned with inventory allocations within the uncertainty set.

A rich variety of bimodal objective functions and models can be analyzed in such an ally-adversary setting. We take one step in this direction by demonstrating that by treating the degree of optimism, that we denote by λ , as a machine-learning hyper-parameter, one can gainfully identify a data-driven tradeoff between the best- and worst-case demand scenarios. The resultant demand pattern is obtained based on the chosen objective and the decision-maker's degree of optimism λ (akin to Kelly's investment fraction f) and will lie in between the two extremes of best- and worst-case demands. We describe our canonical approach below. See Appendix B for alternative ways to exploit a location-specific information edge.

Let us denote the allied best-case demand by \mathbf{D}^+ and the adversarial worst-case demand by \mathbf{D}^- respectively, both in set U , in response to an inventory decision x . We use the optimistic hyper-parameter λ to identify the net demand at any location as a convex combination of best-case and worst-case demand. As U is a polyhedral set, the resultant demand scenario is also in set U . In the proposed (static) Bimodal Inventory Optimization Model (BIO- λ), we identify the inventory decisions along with the optimistic demands jointly in the first stage. In the second stage, we solve a sub-problem similar to RO to identify the adversarial demands for the given allocations and optimistic demands at the fixed λ parameter, and in the third stage, calculate the fulfillment decisions to the resultant demand. We formulate BIO- λ as follows.

$$Z_{SBIO-\lambda}^*(\bar{\mathbf{I}}) = \max_{\mathbf{x}_t \geq 0, \mathbf{D}^+ \in U} \min_{\mathbf{D}^- \in U} \max_{\substack{\{\mathbf{s}_t, \mathbf{y}_t, \mathbf{I}_{t+1}\} \in \\ F(\mathbf{I}_t, \lambda \mathbf{D}_t^+ + (1-\lambda)\mathbf{D}_t^-, \mathbf{x}_t)}} \sum_{t \in \mathcal{T}} O(\mathbf{s}_t, \mathbf{y}_t, \mathbf{I}_{t+1}, \lambda \mathbf{D}_t^+ + (1-\lambda)\mathbf{D}_t^-, \mathbf{x}_t) \quad (4.11)$$

If λ is zero, we retrieve the original adversarial RO model (i.e., RO/pure RO is the same as BIO-0). From a computational perspective, static BIO- λ is identical in complexity to the static

pure RO problem. In particular, the optimistic part of the problem (finding \mathbf{D}^+) is a relatively easy problem and is jointly solved with allocation, and requires no additional information beyond what is already specified for the pure adversarial part of the problem. Section 5 describes our solution strategy for the BIO model.

For a given allocation x , the best-case outcome for problem $BIO - 1$ occurs when the demand is maximally aligned with the inventory distribution across locations (demand as close to the inventory levels as possible) and the worst-case is when demand is maximally mis-aligned with the inventory (i.e., high demands when there is little or no inventory and vice-versa). See Appendix C, for a closed form solution of BIO-0 and BIO-1 for a single walk-in location setting. The following theorem provides insight into the structure of the $BIO - \lambda$ solution and connects the best- and worst-case solution via a λ -superposed line segment.

THEOREM 1. *Given λ , there exists an $x_{BIO-\lambda}^*$ such that $x_{BIO-\lambda}^* = \lambda x_{BIO-1}^* + (1 - \lambda)x_{BIO-0}^*$ and the corresponding optimal objective value $Z_{BIO-\lambda}^*$ satisfies $Z_{BIO-\lambda}^* = \lambda Z_{BIO-1}^* + (1 - \lambda)Z_{BIO-0}^*$. In other words, for any given λ , there exists an optimal allocation for $BIO - \lambda$ that is a linear superposition of the respective optimal quantities for the best case scenario (when $\lambda = 1$, i.e., $BIO - 1$) and the robust scenario (when $\lambda = 0$, i.e., $BIO - 0$). Moreover, the optimal objective value follows the same superposition structure.*

This theorem shows that the $BIO - \lambda$ problem can be decomposed into independent best- and worst-case problems that could be easily recombined. This suggests an alternative computational strategy of first solving the independent problems (just once) and thereafter one can simply superpose these solutions for any λ . Table 2 summarizes the results for a 3-location network having only walk-in demands that empirically demonstrate that the optimal allocation to the BIO- λ problem is a superposition of the best and worst cases.

The questions that remain are (1) how does a BIO solution for a chosen λ perform in a Monte-Carlo simulation and (2) how should this performance be measured? The above theorem suggests that we can perform a one-dimensional search over $\lambda \in [0, 1]$, where each value corresponds to a

Setting	p = 0, b = 160		p = 160, b = 0		p = 80, b = 80	
	Allocation	Estimated Obj	Allocation	Estimated Obj	Allocation	Estimated Obj
Pure RO	[3,3,3]	-360	[1,1,1]	40	[1.75,1.75,1.75]	-130
Optimistic	[1,0,0]	-40	[3,3,0]	720	[3,3,0]	240
BIO-25%	[2.5,2.25,2.25]	-280	[1.5,1.5,0.75]	210	[2.0625,2.0625,1.3125]	-37.5
BIO-50%	[2,1.5,1.5]	-200	[2,2,0.5]	380	[2.375,2.375,0.875]	55
BIO-75%	[1.5,0.75,0.75]	-120	[2.5,2.5,0.25]	550	[2.6875,2.6875,0.4375]	147.5

Table 2 Example of Theorem 1 in a symmetric 3-location walk-in only setting with $L = 0$, $h = 0$, $c = 40$ and

$$U = \{(d_1, d_2, d_3) | 0 \leq d_i \leq 3 \forall i = 1, 2, 3; \text{ and } 1 \leq d_1 + d_2 + d_3 \leq 6\}.$$

BIO- λ allocation, ensuring an approach that maintains data-driven and distribution-free properties.

We formalize this result as a corollary without proof and is immediate from Theorem 1.

COROLLARY 1. *Given a data set from U , identifying the sample optimal λ^* that optimizes for a user-specified objective function (e.g., SAA) reduces to a single-dimensional optimization problem using x_{BIO-0}^* and x_{BIO-1}^* . For a convex objective, it reduces to a bisection search on the $\lambda \in [0, 1]$ line segment.*

Note that this approach may not yield the globally optimal solution for the user-specified objective, as achieving true optimality may require knowledge of the underlying distribution or access to a large dataset or may need a location-specific λ describe in Appendix B. Instead, it offers a simple, data-driven, distribution-free method that approximately optimizes the chosen objective by assessing out-of-sample performance on a relatively small validation set. This stands in contrast to the larger training dataset typically required to compute an exact SAA solution, for example, that maximizes mean returns (Kleywegt et al. 2002, Bertsimas et al. 2018). Using BIO, one could aim to balance optimistic and pessimistic (conservative) scenarios via out-of-sample analysis—enhancing average-case performance while preserving robustness.

The proposed BIO methodology is not restricted to inventory problems and can be applied to any compatible scarce resource allocation problem where RO is viable while noting that the above results may need to be validated in other settings.

Next we expand on the BIO- λ formulation. In the general case, we will have to introduce allied demands in all channels as discussed in the formulation (4.11). Noting the lop-sided impact of the adversary on the channels, we limit the allied demands to the walk-in channel only as it does not have a recourse opportunity. As our chosen uncertainty set U can be decomposed by channel, we are easily able to apply this restriction. The resultant BIO formulation exhibits a multi-class demand structure as shown below.

$$\begin{aligned} Z^{SBIO-\lambda}(\mathbf{I}) = & \max_{(x,s^+) \geq 0, \mathbf{D}^+ \in U} \min_{\mathbf{D}^- \in U} \max_{(s^-, y, I) \geq 0} \sum_{t \in \mathcal{T}} \sum_{l \in \Lambda} \left[(p_{tl}^b + b_{tl}^b)(s_{tl}^{b+} + s_{tl}^{b-}) - b_{tl}^b(\lambda D_{tl}^{b+} + (1-\lambda)D_{tl}^{b-}) \right] \\ & + \sum_{t \in \mathcal{T}} \sum_{z \in Z} [(p_t^o + b_t^o - c_{lz})y_{tlz} - b_t^o D_{tz}^{o-}] - \sum_{t \in \mathcal{T}} \sum_{l \in \Lambda} [h_l I_{t+1,l}^0 + C_l x_{tl}] \end{aligned} \quad (4.12)$$

$$\text{subject to. } s_{tl}^{b+} \leq \lambda D_{tl}^{b+} \quad \forall l \in \Lambda, t \in \mathcal{T}$$

$$s_{tl}^{b-} \leq (1-\lambda)D_{tl}^{b-} \quad \forall l \in \Lambda, t \in \mathcal{T} \quad (4.13)$$

$$\sum_{l \in \Lambda} y_{tlz} \leq D_{tz}^{o-} \quad \forall z \in Z, t \in \mathcal{T} \quad (4.14)$$

$$s_{tl}^{b+} + s_{tl}^{b-} + \sum_{z \in Z} y_{tlz} + I_{t+1,l} = I_{tl} + \bar{I}_l^{t+1} \mathbb{1}_{t < L_l} + x_{t-L_l,l} \mathbb{1}_{t \geq L_l} \quad \forall l \in \Lambda, t \in \mathcal{T} \quad (4.15)$$

$$I_{0l} = \bar{I}_l^0 \quad \forall l \in \Lambda. \quad (4.16)$$

We write separate sales constraints for the optimistic and pessimistic part of the demand vector by creating corresponding optimistic and pessimistic terms in the objective function.

Next, we provide comparative insight into the optimal solution structure of the (static) unimodal RO strategy versus its bimodal counterpart using a simple example (leveraging the cut-generation approach in Section 5). We constrain the allocations to be integer-valued in these experiments. While the alternative scoring objectives continue to lie in between the best and worst case, we cannot fully exploit the results of Theorem 1 as the allocation space is now discrete. We simply re-solve the BIO- λ problem for varying λ and use out-of-sample data to identify a preferred λ .

EXAMPLE 1. Consider an omnichannel retailer with nodes, zones, fulfillment costs, uncertainty set and the true unknown demand distributions as depicted in Fig. 1. Suppose also $L = 0$.

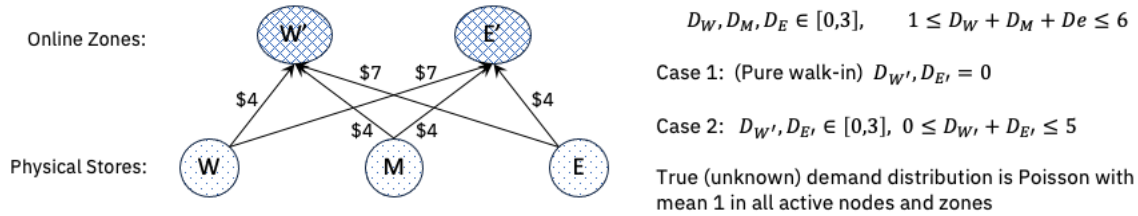


Figure 1 Example of an omnichannel retailer.

Method	Reco. Allocation	Est. best-worst case	Est. Worst Case	Est. Worst Case Obj	Est. Obj	Rlze. Min.	Rlze. 5th percentile	Rlze. 10th percentile	Rlze. Median	Rlze. Max.	Rlze. Mean
Pure RO	[3,3,3]	-	[3,3,0]	-360	-360	-1000	-520	-360	-360	-360	-372.32
BIO-50%	[2,2,2]	[0,0,1]-[3,3,0]	[3,3,0]	-560	-240	-1040	-560	-400	-240	-240	-291.04

Table 3 Example of the recommend allocation and profit statistics of pure RO and BIO in the walk-in only setting. Allocation (alternatively, demands) are specified for nodes in the following sequence [M,W,E]. Expansion of the acronyms used in the table include Reco. for Recommended, Est. for Estimated and Rlze. for Realized.

In Table 3, we summarize the results (allocations, estimated objectives and their corresponding worst case/best-worst case demands scenarios) of the pure walk-in setting described in case 1 of Fig. 1 when $p = h = 0$, $b = 160$ and $c = \$40$ for the pure RO and BIO-50% methods. Observe how the pure RO model invests in a lot inventory (9 units) to maximally reduce lost sales penalty, while the BIO model invests just 6 units. Table 3 also includes the realized statistics of the objective obtained from a Monte Carlo simulation run on 1000 samples. Note that the estimated worst case and the simulated worst case profitability values do not match as the robust model assumes a finite polyhedral set to capture the most commonly occurring scenarios, as opposed to the unbounded Poisson distribution used by the simulation engine. Observe how the BIO model trades off worst-case performance (7.7%, 11.1% at the 5th, 10th quantile) compared to pure RO to improve the average case (21.8%).

In Table 4, we provide results for a more general scenario with e-commerce demands, case 2 in Fig. 1, when (1) $p = 0$, $b = 160$ and (2) $p = b = 160$, where $c = 40$ and $h = 0$. Besides the pure RO, BIO- λ for a few different values of λ , we also include a baseline method, PWL which is a deterministic piece-wise linear network model described in Section 6.2. For ease of visualization,

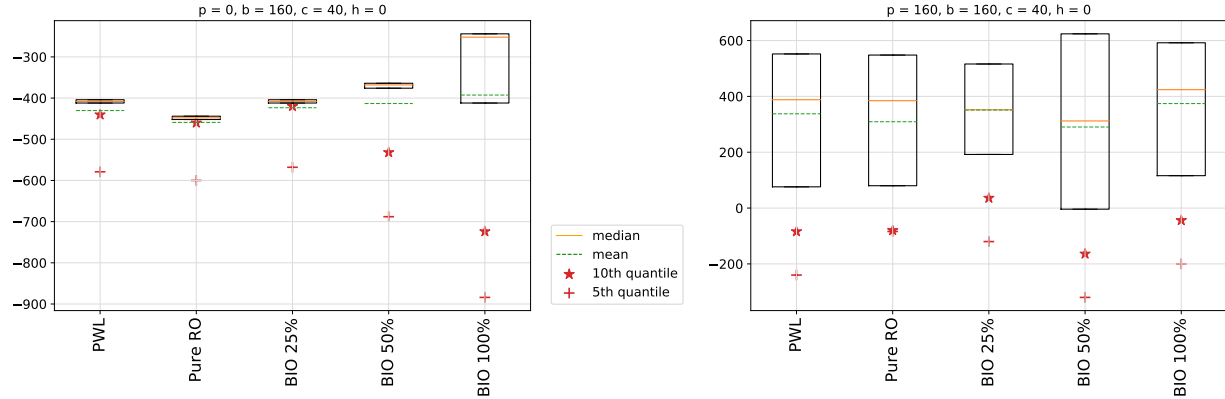


Figure 2 The realized profitability box plots across different methods in case 2 of example 1.

Setting	$p = 0, b = 160, c = 40, h = 0$					$p = 160, b = 160, c = 40, h = 0$				
	PWL	Pure RO	BIO 25%	BIO 50%	BIO 100%	PWL	Pure RO	BIO 25%	BIO 50%	BIO 100%
Reco. Allocation	[2,4,4]	[5,3,3]	[4,3,3]	[5,2,2]	[3,1,2]	[2,4,4]	[2,2,2]	[2,3,2]	[4,3,1]	[3,3,3]
Est. Best-Worse Case	-	-	[0,.5,.5]-	[0,1,0]-	[0,1,0]-	-	-	[2,3,1]-	[3,3,0]-	[3,3,0]-
Est. Worst Case	[3,3,0][3,2]	[3,3,0][3,2]	[3,3,0][3,2]	[0,3,3][3,2]	[0,3,3][3,2]	[3,0,0][0,0]	[3,0,3][3,2]	[0,1,0][0,0]	[0,0,3][0,0]	[0,1,0][0,0]
Est. Worst Case Obj	-586	-463	-579	-700	-1052	-240	-88	-120	-480	-200
Rlze. Minimum	-1551	-1420	-1540	-1652	-2008	-400	-1052	-776	-640	-360
Rlze. 5th percentile	-579	-600	-568	-688	-884	-240	-84	-120	-320	-200
Rlze. 10th percentile	-547	-460	-420	-532	-724	-84	-80	36	-164	-44
Rlze. Mean	-430	-459	-423	-413	-393	338	309	351	290	374
Rlze. Median	-408	-448	-408	-368	-252	388	385	352	312	424

Table 4 The recommend allocation and profit statistics across different methods in case 2 of example 1.

Allocation/demands are specified for nodes/and zones in the sequence $[M,W,E]/[M,W,E][W, E]$ respectively.

In Fig. 2 we plot the realized profitability from the Monte Carlo simulation. We observe that a BIO-25% improves the mean profitability and the robustness by 7.8% and 5.3% (at 5th quantile) respectively over pure RO when $p = 0$ and trades off profitability against robustness (improves former by 13.5% and drops latter by 42.8% but changes direction and improves by 45% at the 10th quantile) when $p = 160$. In both these examples, we observe that the PWL baseline is competitive and outperforms pure RO across many metrics (5th, 10th quantiles and average case metrics) while BIO 25% outperforms PWL and RO across all metrics. We also observed this behavior in real client data and is one of the findings that motivated the development of a BIO model. These results

suggest that the benefit of optimism can increase with higher p when the other parameters remain the same. The non-convex behavior in the mean profitability between BIO-50% and BIO-100% when $p=160$ is attributed to the discreteness constraint on allocation.

5. Column and Cut Generation (CCG) Method to solve BIO- λ

We reformulate the inner min-max problem of BIO- λ as a minimization problem by taking the dual of the innermost maximization problem:

$$\begin{aligned} \min_{\mathbf{D}^- \in U, \alpha, \beta \geq 0, \gamma} & \sum_{t \in \mathcal{T}, l \in \Lambda} (1 - \lambda)(\alpha_{tl} - b_{tl}^b)D_{tl}^{b-} + \sum_{t \in \mathcal{T}, z \in Z} (\beta_{tz} - b_t^o)D_{tz}^{o-} + \sum_{l \in \Lambda} \gamma_{0l} \bar{I}_l^0 \\ & + \sum_{t \in \mathcal{T}, l \in \Lambda} \gamma_{tl} (\bar{I}_l^{t+1} \mathbb{1}_{t < L_l} + x_{t-L_l, l} \mathbb{1}_{t \geq L_l} - s_{tl}^{b+}) \end{aligned} \quad (5.1)$$

$$\text{subject to. } \alpha_{tl} + \gamma_{tl} \geq p_{tl}^b + b_{tl}^b \quad \forall t \in \mathcal{T}, l \in \Lambda \quad (5.2)$$

$$\beta_{tz} + \gamma_{tl} \geq p_t^o + b_t^o - c_{lz} \quad \forall t \in \mathcal{T}, l \in \Lambda, z \in Z \quad (5.3)$$

$$\gamma_{tl} - \gamma_{t+1, l} \geq -h_l \quad \forall t \in \mathcal{T}, l \in \Lambda \quad (5.4)$$

$$\gamma_{T, l} = 0 \quad \forall l \in \Lambda \quad (5.5)$$

Observe that both \mathbf{x} and the optimistic walk-in sales variable s_{tl}^{b+} are passed on to this problem, which we henceforth refer to as the sub-problem (SP). The variables α, β and γ are the duals to the constraints in the primal problem (the innermost fulfillment problem). The inner problem in the above model is nonlinear and NP-Hard due to the bi-linear terms $\alpha_{tl}D_{tl}^{b+}$, $\beta_{tz}D_{tz}^o$. We aim to leverage the column and cut generation (CCG) algorithmic framework to solve two-stage RO problems proposed by Zeng and Zhao (2013). The CCG algorithm guarantees optimal convergence if the subproblem is solved exactly. To achieve the latter, we propose an exact mixed-integer linear reformulation that relies on the proposition below and the fact that there exists an optimal (worst-case) sub-problem demand \mathbf{D}^- which is at an extreme point of the uncertainty set U (given the dual variables α, β, γ , the problem is an LP with \mathbf{D}^- as the variables).

PROPOSITION 1. *The extreme points of the uncertainty set U described in Eq.(3.1) are integral with integral bounds.*

The proposition states that so long as the bounds in Eq.(3.1) (which are quantiles) are integral, the extreme points are integral. Real-world demand realizations are discrete and therefore, the estimated quantiles of demands, and their aggregate values, are integral, making it easier to fulfill the conditions of the proposition. For general uncertainty sets U whose structure may be different from Eq.(3.1), the results of the proposition may not be true. In that case, one may choose to work with (1) a discrete uncertainty set, say U_Z , or (2) the convex set generated by the integral points in U . Next, we propose an exact mixed-integer linear reformulation by leveraging the discreteness of the optimal adversarial demand. Specifically, we enumerate all integral values within the uncertainty set U which happens to also include the optimal adversarial demand, due to Proposition 1.

PROPOSITION 2. *The sub-problem can be re-formulated exactly as follows. Here, let \bar{D}_{tlk}^b for $k \in K_{tl}^b$ and \bar{D}_{tzk}^o for $k \in K_{tz}^o$ be the discrete values of the uncertainty that are feasible to the first set of box constraints in Eq. (3.1) in set U and $M = \max_{t,l} \{p_{tl}^b + b_{tl}^b, p_t^o + b_t^o - c_{tz}\} + |T + 1| \max_l h_l$.*

$$Z^{SP(\mathbf{x}, \mathbf{s}^{b+})} = \min_{\substack{\alpha, \alpha^*, \beta, \beta^* \geq 0, \\ \gamma, w \in \{0,1\}}} \sum_{\substack{t \in \mathcal{T}, l \in \Lambda, \\ i \in I_{tl}^b}} (1 - \lambda_t) \bar{D}_{tlk}^b (\alpha_{tlk}^* - b_{tl}^b w_{tlk}^b) + \sum_{\substack{t \in \mathcal{T}, z \in Z, \\ i \in I_{tz}^o}} \bar{D}_{tzk}^o (\beta_{tzk}^* - b_t^o w_{tzk}^o) \\ + \sum_{l \in \Lambda} \gamma_{0l} \bar{I}_l^0 + \sum_{t \in \mathcal{T}, l \in \Lambda} \gamma_{tl} (\bar{I}_l^{t+1} \mathbb{1}_{t < L_l} + x_{t-L_l, l} \mathbb{1}_{t \geq L_l} - s_{tl}^{b+}) \quad (5.6)$$

$$\text{subject to.} \quad \text{Eqs. (5.1), (5.3), (5.4), (5.5)} \quad (5.7)$$

$$\alpha_{tlk}^* \leq M w_{tlk}^b; \quad \beta_{tzk}^* \leq M w_{tzk}^o \quad \forall t \in \mathcal{T}, l \in \Lambda, z \in Z, i \quad (5.8)$$

$$\sum_{k \in K_{tl}^b} \alpha_{tlk}^* = \alpha_{tl}; \quad \sum_{k \in K_{tz}^o} \beta_{tzk}^* = \beta_{tz} \quad \forall t \in \mathcal{T}, l \in \Lambda, z \in Z \quad (5.9)$$

$$\sum_{k \in K_{tl}^b} w_{tlk}^b = 1; \quad \sum_{k \in K_{tz}^o} w_{tzk}^o = 1 \quad \forall t \in \mathcal{T}, l \in \Lambda, z \in Z \quad (5.10)$$

$$\bar{D}_t^{oL} \leq \sum_{z \in Z, k \in K_{tz}^o} \bar{D}_{tzk}^o w_{tzk}^o \leq \bar{D}_t^{oU} \quad \forall t \in \mathcal{T} \quad (5.11)$$

$$\bar{D}_t^{bL} \leq \sum_{l \in \Lambda, k \in K_{tl}^b} \bar{D}_{tlk}^b w_{tlk}^b \leq \bar{D}_t^{bU} \quad \forall t \in \mathcal{T} \quad (5.12)$$

Note that M can be tightened by having it tailored by time period and node or zone in an actual implementation (see appendix). Our method capitalizes on the discrete nature of the optimal

uncertainties and employs the Relaxation and Linearization Technique (RLT, Sherali and Adams 1998) to exactly re-formulate the sub-problem as an MIP. This contrasts with traditional methods such as those in Zeng and Zhao (2013), Bertsimas and Shtern (2018), which linearize the KKT conditions under continuous uncertainty assumptions using generic big-M parameters to derive MIP reformulations, or the approach in Simchi-Levi et al. (2019), which leverages integral coefficients for network flow problems to construct MIP reformulations.

Propositions 1 and 2 together establish that the sub-problem for the BIO formulations can be solved exactly with MIP solvers despite being NP hard. The CCG algorithm converges to the optimal solution in finite iterations as long as the sub-problem is solved exactly (Zeng and Zhao 2013). To solve two-stage RO problem, we integrate the MIP sub-problem within the CCG algorithm. Here, the master problem is formulated using only a finite set of feasible \mathbf{D}^- uncertainty values, but with a structure identical to the original problem. The solution method can be viewed as the master generating a sequence of beneficial allocations, and the sub-problem adding corresponding adversarial demand ‘cuts’ to master and the iterations stop when the two problems converge in their achieved objectives. In the interest of brevity, we include the master problem formulation and the corresponding CCG algorithm’s adaptation to the BIO- λ problem in Appendix G.

6. Computational Experiments

In this section, we use real-life data to compare the practical performance of different inventory optimization policies developed in this paper relative to baseline methods, and analyze their impact on total profitability and other metrics.

We obtained data from a leading omnichannel retailer operating over 150 locations and multiple DCs (warehouses) in the continental United States. The dataset includes historical sales records from transaction-log and e-commerce orderline data, meta-data such as product and location attributes, and rate cards used for calculating the fulfillment costs. All locations are SFS equipped, i.e., their store inventory can be used to fulfill online orders. We selected four jackets subcategories in the apparel category during the second sales peak (the first being the holiday

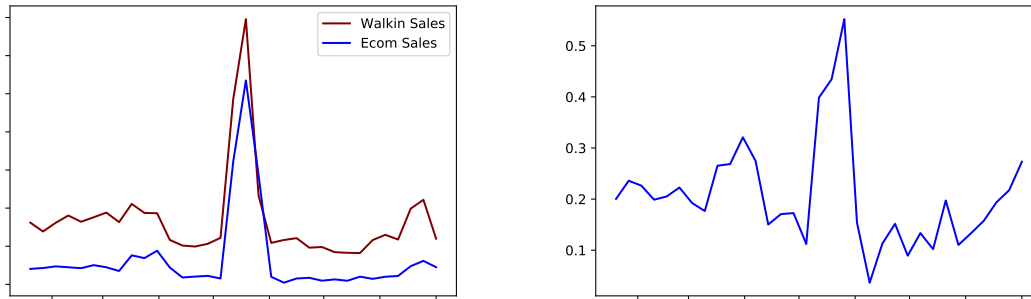


Figure 3 Actual sales trends by channel (left) and the actual e-commerce sales fraction of the total sales (right) for select SKUs around sales peak.

season) of the calendar year. We analyze 23 SKUs corresponding to the top 5% best-sellers that account for more than 45% of the total sales volume during the 3 week testing period. Fig. 3 depicts the chain-level sales and the corresponding e-commerce share for these select SKUs over a 3 month peak period. Over 60% of these sales occur during the testing period. The spike in walk-in and e-commerce sales (and the e-commerce share) during this peak underscores the need for accurate inventory positioning to meet omnichannel demands as it can significantly impact the retailer margins for the entire season.

We assume a weekly replenishment cycle and a lead time of one-week.

6.1. Inputs for inventory management

We cluster the individual zip3 sales across the continental US into 22 zones based on similar node-to-zip3 lowest unit fulfillment costs in order to deal with the low sales rate at the zip3 level. The labor cost by origin node (lower in DCs compared to metropolitan area) are additionally incorporated to obtain the total fulfillment cost.

We employ a time-series multi-task uncensored demand forecasting model at the SKU-location-channel-week level with hierarchical location-based reconciliation to generate a daily refresh of the mean weekly demand forecast for the next few weeks. Specifically two neural network-based models, one for SKU-store-Demand-week forecasts, and the other for SKU-zone-OnlineDemand-week predictions were developed using 18.7 and 3 million observations respectively corresponding to daily observations between 2016 to 2019 for SKUs in the chosen sub-categories across locations

and zones. Multi-tasking allows the model to learn across multiple time-series based on common attributes (common sub-patterns in hierarchies and corresponding historical sales, prices, and calendar and seasonal attributes) under sparse data conditions and captures correlations automatically. Sales data is uncensored within this procedure to account for lost sales due to stock-outs and produce an unconstrained demand forecast. Reconciliation ensures consistency between chain-level and location-specific forecasts, an aspect that is important in our problem context. The forecasting model minimizes a Poisson loss function (along with the regularization and incorporation hierarchical aggregate series) keeping in mind the low rate of sales and the discreteness of demand, among other factors. This loss function also enables us to aggregate the local mean demands into a chain-level mean demand.

To generate the required local and chain level quantiles of the uncertainty set, we use the 5th and the 95th quantile of the Poisson distribution. For Monte Carlo sample paths, we use a random number generator with an underlying Poisson distribution with the estimated mean. To be distribution-free, a quantile loss function at multiple levels of the hierarchy could be alternatively used instead of the Poisson loss function. We adopt the former approach to be consistent in our modeling and our sample generation procedure as Monte Carlo samples are required for the out-of-sample computational comparisons we perform in this paper.

6.2. Baseline Inventory Optimization Methods

Three fast heuristic methods described below are used to generate the baseline KPIs for comparison. The methods rely on location-specific demand quantiles, evaluated using an assumed distribution—Poisson for perfect information and Uniform for imperfect information. The critical-quantile we use is the location-channel specific ratio of the margin (price less the item cost, and less the average shipping cost for the ecommerce channel) to the price of the item.

1. *Basestock-based distribution heuristic:* We use the basestock heuristic to order supply at each store location for walk-in demand and next at the chain level for online demand. In the latter case, we consider the warehouse inventory as well as excess inventory in stores (i.e., that

above critical-quantile store demand) to derive the current inventory position. The chain level e-commerce supply is distributed amongst warehouses in-proportion to their individual basestock order quantities (where in, demand is obtained by mapping zones to their nearest warehouses).

2. *Piecewise-linear (PWL) network-based heuristic:* We extend the deterministic version of the pure robust model to allow for two classes of demand at each location: the mean demand, and the excess beyond the mean and up to the critical quantile (if higher). The price and penalties for the second class are associated with a discount factor that is calibrated to prioritize the satisfaction of all mean demands over any excess.
3. *Basestock-based network distribution heuristic:* This heuristic resembles the basestock heuristic described above but differs in key aspects. Instead of pooling online orders at the chain level, it pools demand network-wide, ordering only the incremental quantity beyond walk-in orders for online demand. The additional supply is then split, with a fraction θ allocated to stores and the rest to warehouses. Within each group, the distribution across nodes is proportional to their respective base-stock order quantities, where DC demand is obtained by mapping zones to their nearest warehouses. The incremental order quantity for online demand is capped so it does not exceed what would result from pooling at the chain level¹.

For the basestock heuristics, we use a capped variation that limits the order quantity to the cycle safe stock level, as it known to outperform the vanilla variant in lost sales settings (Xin 2021). This observation holds across all our experiments, so we adopt it as the default. The heuristic methods do not rigorously model demand uncertainty but instead incorporate its key elements in a practical manner, serving as competitive benchmarks for the real-data sets analyzed (as we will see). Unlike the RO and BIO models, these heuristics do not guarantee feasible solutions in the presence of side-constraints, often required in practical applications, such discussed in Section 4.

¹This restriction is necessary because, for low-sales-rate items, pooling at the network level across thousands of stores could generate excessive incremental demand—mainly for walk-ins that were not driven by store-level orders—resulting in unsold inventory and subpar performance.

6.3. Experimental design and setup

We perform two different computational experiments under various initial conditions and parameter settings to assess the performance of the inventory management policies and their suitability for real-world applications. The first experiment involves a batch Monte-Carlo simulation, where the optimizer is executed only once to evaluate its performance in isolation across various scenarios. The second experiment is a business value assessment over an extended time horizon using a transaction-level Monte Carlo simulation. Here, the inventory optimizers were executed on a weekly basis, and demands were fulfilled order-by-order on-the-fly. This simulation mimics a real-life order fulfillment system.

A two-week planning horizon is used for all the inventory optimizers in both experiments. As we solve several large instances of the two-stage inventory optimization model which involve NP-hard sub-problems, we employ a heuristic version of Algorithm 1, by employing an *alternating heuristic* (AH) to warm start and polish the sub-problem solution along with practical safeguards to limit the maximum run time (300 seconds) and the number of Benders iterations (20). The AH iteratively switches between solving for the duals with fixed demands and then for demand by fixing the dual values at their new values until successive dual solutions converge.

6.3.1. Batch Monte-Carlo simulations with optimizer executed just once: The optimizers are executed for a peak sales week for different hyper-parameter settings and starting inventory positions. We evaluate the resultant allocations of each optimizer by solving the innermost maximization problem described in (4.8) and generate a profitability distribution of the achieved objective using the Monte-Carlo samples.

In the first experiment, we analyze the sensitivity of the profitability gain to the parameter settings by evaluating the gain at three different parameter settings where (1) $p_t = 0, b_t = p_{0t}$, (2) $p_t = p_{0t}, b_t = p_{0t}$ and (3) $p_t = p_{0t}, b_t = 0$, where p_{0t} is the price of the item in week t . For these SKUs, the margin is on average 50% at full price. The SKU prices drop by 20% between the lead time and cycle time week. We assume that $h = 0$. For each of these parameter settings, we

consider three different starting inventory positions to recreate different network conditions: (1) zero - all locations have zero inventory; (2) mean - all locations have inventory equal to mean of the lead time demand including DCs that have the preferred zones mapped to them; and (3) excess - DCs have excess inventory by SKU, and stores have inventory that is sufficient at the category level but is imbalanced across SKUs and locations (inventory equal to total mean walk-in demand is randomly allocated across SKUs and stores). We implement the aforementioned baseline methods—Basestock, PWL, and BS Net θ —under perfect distributional information (i.e., Poisson) and apply the network heuristic under imperfect distributional information (i.e., Uniform), denoted as BSU Net θ . We evaluate $\theta = 0$ and $\theta = 1$ to analyze the impact of network pooling and the incremental value of maintaining this inventory at stores². Additionally, we evaluate distribution-free BIO models for different λ values (denoted by BIO 5%, BIO 10%, BIO 25%, BIO 50% and BIO 75%), and BIO-0, i.e., the pure robust method (Pure RO).

For the BIO model analysis, we split the (1000) Monte Carlo samples into a cross-validation (80%) and a hold-out test data set (20%). Doing so enables us to identify the most profitable $BIO - \lambda$ on average at the SKU level via a one-dimensional grid search (across λ in $\{5, 10, 25, 50, 75\}$) using the cross-validation data set and evaluate performance of this optimized $BIO - \lambda$ on the hold-out data. We refer to this ML based BIO model as ‘BIO-best’. For appropriate comparison, results of all models are reported on the hold-out data only.

Fig. 4 provides the total ordering decision per node type and resulting profitability distribution for various settings and methods aggregated over all SKUs. Table 5 complements this by reporting the percentage improvement in mean profitability gains compared to the basestock method. The 5th quantile percentage gains closely follow the insights from mean performance gains, also as illustrated in Fig. 4, so we do not report them separately.

Referring to Table 5, we observe that under perfect information, the capped basestock network heuristic significantly outperforms the vanilla basestock approach when $\theta = 1$ in both the mean and

² Since $\theta = 1$ consistently gave near-optimal results when tuned, we present only this case.

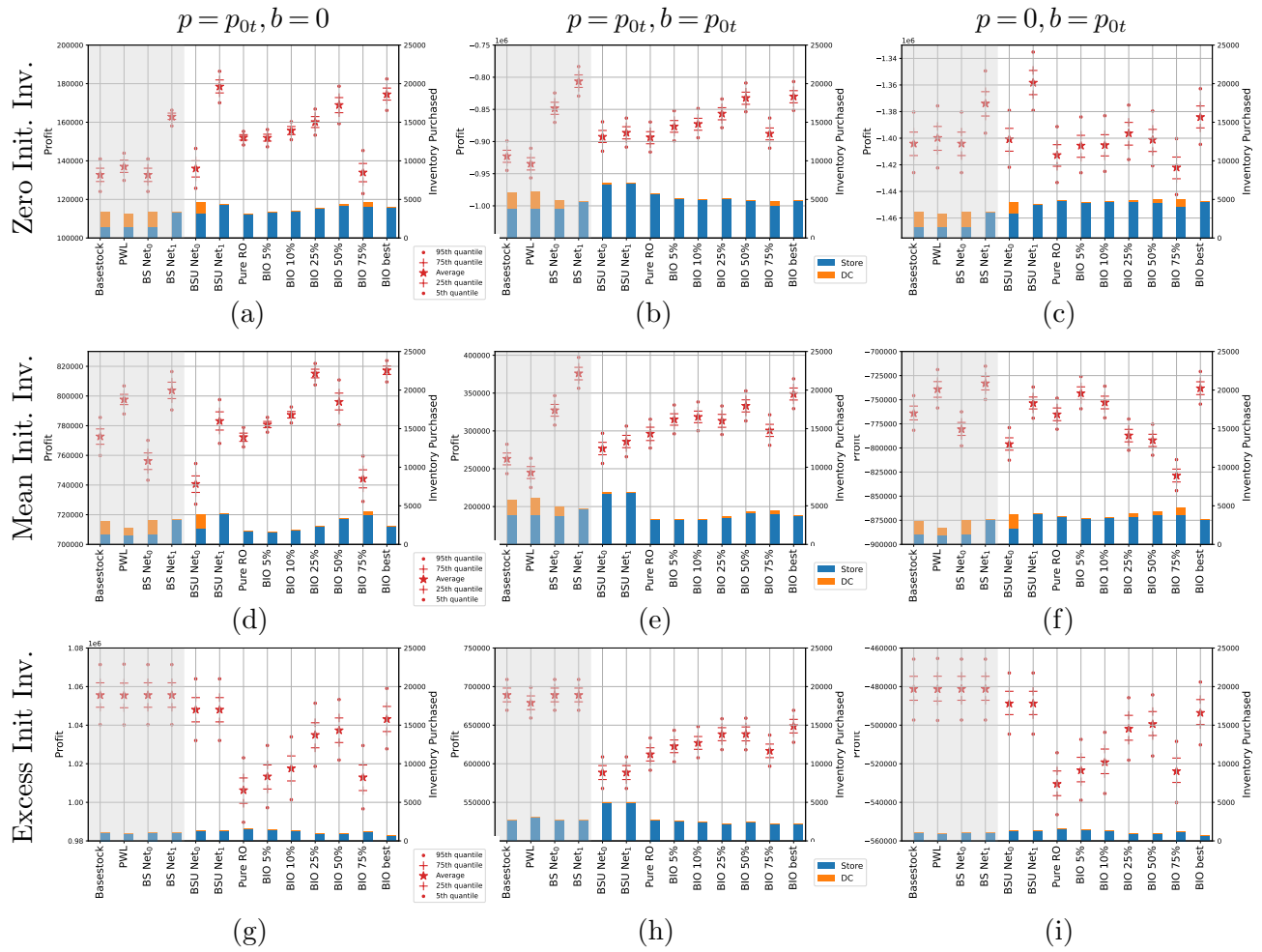


Figure 4 Total inventory allocation across stores and DCs and resultant total profitability distribution in the Monte Carlo simulation. Initial Inventory is zero in (a-c), mean in (d-f), and excess in DC in (g-i). Price and back order penalty multipliers (p, b) to the weekly item price are: $p = 1, b = 0$ in (a,d,g), $p = 1, b = 1$ in (b,e,h) and $p = 0, b = 1$ in (c,f,i). Grey-shaded settings: perfect distributional info; others: imperfect or distribution-free.

zero-inventory settings, highlighting the single-channel method’s inability to effectively leverage cross-channel inventory. However, for $\theta = 0$, this advantage is only observed when $p = b = 1$. This occurs because, in low sales-rate settings (even during a peak week), lower demand quantiles (when $p = 0$ or $b = 0$) lead to negligible order quantities, often zero. A slight increase in inventory at stores improves results, which explains the superior performance at higher quantiles (when $p = b = 1$ or when $\theta = 1$). This same reasoning explains why, under imperfect information (Uniform distribution), the capped heuristic performs better in the zero-inventory case. Across all settings, we note that when incremental online inventory pooled at the network level is pushed to stores

Initial Inv.	Price	Lost Sales	Perfect Distr. Info.			Imperfect Distr. Info.		Distribution-free					
			Setting	Factor	Factor	PWL	BS Net ₀	BS Net ₁	BSU Net ₀	BSU Net ₁	Pure RO	BIO 5%	BIO 10%
Zero	1	0	3	0	23	2	34	15	14	17	21	27	31
Zero	1	1	-1	8	13	3	4	3	5	5	7	10	10
Zero	0	1	0	0	2	0	3	-1	0	0	1	0	1
Mean	1	0	3	-2	4	-4	1	0	1	2	5	3	6
Mean	1	1	-7	24	43	5	9	13	20	21	19	27	33
Mean	0	1	3	-2	4	-4	1	0	3	1	-3	-4	3
Excess	1	0	0	0	0	-1	-1	-5	-4	-4	-2	-2	-1
Excess	1	1	-1	0	0	-15	-15	-11	-10	-9	-7	-7	-6
Excess	0	1	0	0	0	-2	-2	-10	-9	-8	-4	-4	-3

Table 5 Percentage improvement of the mean total profitability over the perfect info. basestock heuristic.

($\theta = 1$), both channels benefit, enhancing overall performance. All gains disappear in the excess inventory setting, as the problem simplifies to a single-channel in-store allocation problem that is separable by location. For each individual problem, the basestock method is known to be optimal for maximizing mean profitability.

While the perfect-information basestock network heuristic outperforms the imperfect-information and distribution-free settings, its advantage diminishes in realistic scenarios where demand distribution information is inherently imperfect. Therefore, for a practical comparison, we evaluate the imperfect distribution setting against BIO, a distribution-free approach. Across the zero, mean, and excess inventory settings, BIO-best outperforms BSU Net $_{\theta=1}$ (network basestock counterpart) heuristic by 0.4%, 10.1%, and 2.4%, respectively, on average across price settings, resulting in an overall average gain of approximately 4.3%. Notably, we observe significant gains in the $p = b = 1$ setting as well as across all mean inventory settings (average +9%, in 5 of 9 settings), while performance remains relatively low negative otherwise (average -1.6%, in the rest).

We also observe that the pure RO method under-performs relative to the baselines in many parameter regimes. However, this performance gap is closed with a simple tuning of λ via the BIO strategy (also as illustrated in Example 1). This BIO tuning is essential for data-driven distribution-free approaches to effectively compete against simple baselines (serving as an alternative to a full-scale SAA approach, which would require a large number of demand scenarios—potentially

correlated across all locations and channels—leading to both computational challenges as well as difficulties in scenario generation). Specifically, we observe the BIO models with $\lambda > 0$ enhance the performance of the pure RO models on average by 5-6% (with BIO 10%, 25%) which increases to 12% by tuning λ for each SKU using BIO-best. From Fig. 4, we observe that a gradual increase in λ leads to an increase in mean profitability without compromising practical robustness. BIO-best does achieve the best overall performance across the mean and the lower quantiles amongst all the BIO models. The out-of-sample performance worsens when we employ overly optimistic BIO settings (e.g., $\lambda > 50\%$), indicating that a pragmatic range of smaller λ values are preferable.

From Fig. 4, we observe that the ordering policy of the baseline models is invariant to $p + b$ but this is not the case for the robust models. The worst case demand magnitude tends to be large for high b and relatively low for high p . We observe the same trend in the quantity of inventory purchased especially by pure RO models. A key finding to highlight is that across all the omnichannel settings, the best BIO and RO models organically pool inventory by effectively fulfilling walk-in and online demand using inventory at the store (indicated by a thin sliver or lack of an orange bar in Fig. 4 subplots a-f, which denotes the quantity allocated to the DCs).

The average run time across pure RO (unimodal strategy using $\lambda = 0$) and various BIO instances ($\lambda > 0$) are similar as they employ the same run time and iteration limits. We observe an average (\pm standard deviation) run time of 53 ± 28 seconds with 15 ± 3 Benders iterations.

6.3.2. Business Value Assessment: We use the different inventory models to derive a replenishment policy that is executed weekly in tandem with a fine-grained customer transaction level Monte-Carlo simulator that generates sample paths to evaluate various KPIs. This experiment replicates a real-world setting wherein individual walk-in and online orders are individually processed in the order in which they arrive. Daily customer-level orders are generated via an appropriate spread-down of week-location-level demands. Walk-in orders are met first, and e-commerce orders are processed next based on the cheapest fulfillment cost from a tiered set of origin nodes. The tiered node sets are created based on the inventory available to meet the mean daily predicted walk-in demand prior to the next replenishment.

We execute the what-if planner every week over a rolling horizon (the 3-week peak period) for 30 Monte Carlo sample paths. While the first standalone experiment required one optimization instance per SKU (23 instances in total), we now solve 30 optimization instances per SKU per week over the chosen time horizon, yielding a total of $23 \times 30 \times 2 = 1380$ instances; Two consecutive optimization runs are required in a 3 week period because of the one week lead time and noting that the recommended decision in the third week is redundant. We compare the performance of different optimizers: Basestock, PWL, BS Net $_{\theta=0}$, BS Net $_{\theta^*}$, BS Net $_{\theta=1}$, in the perfect distributional information setting, BSU Net $_{\theta=0}$, BSU Net $_{\theta^*}$, BSU Net $_{\theta=1}$, in the imperfect distributional information case, along with pureRO, BIO 10%, BIO 25%, BIO 55% and BIO 50% in the distribution-free case. Here θ^* is obtained via a grid search from 0.6 to 1 in increments of 0.1, and we note that this turn out to be 0.9 and 1 for the perfect and imperfect scenarios respectively. We start with zero inventory in the first week, which automatically translates to an imbalanced mean inventory setting for the following week. The retailer weighed lost sales and achieved sales equally and we employ a price and back order penalty of 1, along with a holding cost of 0 to reflect their preference. The results of the experiments are provided in Fig. 5 and Table 6 respectively.

We observe from Table 6 that in the perfect information setting, the network heuristic outperforms the single-channel heuristic at any value of θ by a significant margin. Specifically, BS Net $_{\theta^*}$ achieves 46% higher profitability than the vanilla basestock policy, highlighting the value of cross-channel inventory management. However, under imperfect information, the profitability of the same network heuristic BSU Net $_{\theta^*}$ decreases by 15% compared to its counterpart BS Net $_{\theta^*}$. For a practical comparison, where demand distribution information is inherently unknown, we evaluate the imperfect information network heuristic, BSU Net $_{\theta^*}$, against the BIO models, which follow a distribution-free approach. We observe that profitability increases by up to 10% and 11% for BIO 25% and BIO 35%, respectively. This gain stems from improved inventory turnover, which increases by approximately 6 points, while the service level declines by 9 percentage points—a trend also observed with the best-case perfect information heuristic, where the service level drops

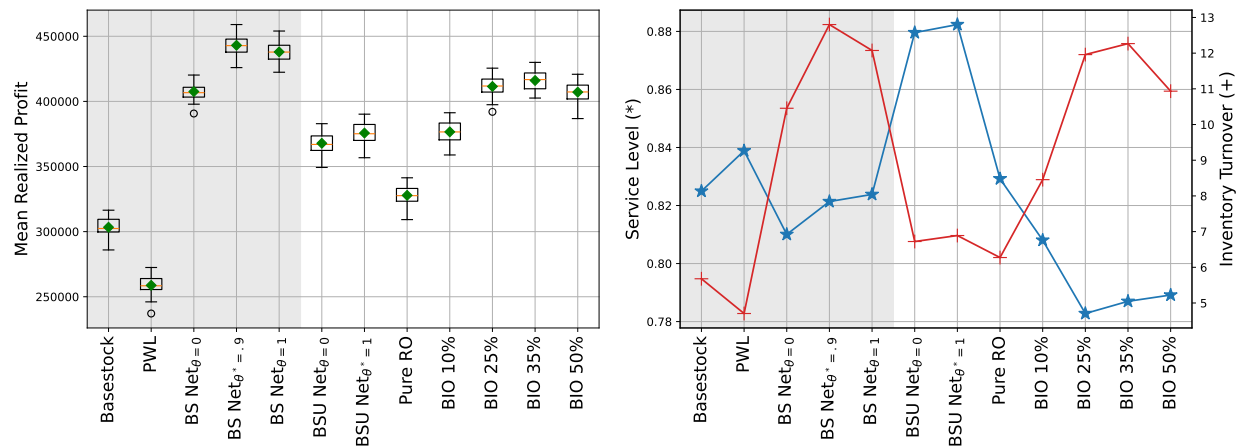


Figure 5 KPIs of different replenishment policies using the transaction-level what-if simulator. Grey-shaded settings assume perfect distributional information; the rest reflect imperfect/distribution-free settings.

Distr. Info.	Optimizer	Replenish Qty	DC Replenish Qty	Walk-in Sales Qty	Total Sales Qty	Ship-from Store Qty	Satisfied Revenue	Shipping Cost	Purchase Cost	Excess Inv. Valued at Cost	E-Com Ser. Lvl.	Total Ser. Lvl.	Inv. Tr.Ov.	Realized Profits
Perfect	Basestock	12,449	2,937	6,390	9,206	59	1,312	13	996	255	0.97	0.82	5.68	303 ± 7
	PWL	13,341	2,955	6,545	9,361	147	1,338	13	1,066	313	0.97	0.84	4.71	259 ± 8
	BS Net _{θ=0}	10,770	1,258	6,224	9,039	1,573	1,285	14	863	135	0.97	0.81	10.46	408 ± 7
	BS Net _{θ*=.9}	10,600	122	6,370	9,166	2,674	1,307	15	849	111	0.96	0.82	12.80	443 ± 8
	BS Net _{θ=1}	10,718	-	6,401	9,193	2,793	1,312	15	859	119	0.96	0.82	12.08	438 ± 8
Imperfect	BSU Net _{θ=0}	12,737	246	7,000	9,815	2,570	1,396	15	1,014	226	0.97	0.88	6.72	368 ± 8
	BSU Net _{θ*=1}	12,706	-	7,032	9,846	2,815	1,402	15	1,011	221	0.97	0.88	6.89	376 ± 8
Distr. free	Pure RO	12,205	43	6,446	9,253	2,764	1,321	15	978	232	0.97	0.83	6.27	328 ± 7
	BIO 10%	11,152	41	6,211	9,017	2,764	1,286	15	894	167	0.97	0.81	8.46	377 ± 8
	BIO 25%	10,198	53	5,927	8,735	2,756	1,244	15	818	113	0.97	0.78	11.96	411 ± 8
	BIO 35%	10,216	91	5,976	8,782	2,715	1,252	15	821	113	0.97	0.79	12.27	416 ± 8
	BIO 50%	10,419	219	5,997	8,806	2,591	1,254	15	832	124	0.97	0.79	10.93	407 ± 8

Table 6 Average observed metrics and KPIs across Monte Carlo scenarios. The units of all revenue, cost and profits are in (K)\$\$. Service level and inventory turnover are referred to as ser. lvl. and inv. tr. ov. respectively.

by 6 percentage points, for a similar increase in inventory turn-over. These results underscore the benefits of network modeling in omnichannel settings, as well as the effectiveness of optimistic-robust methods, which are essential when distributional information is limited or imperfect. In such cases, pure robust models alone fail to achieve competitive performance—BIO 35% yields 27% higher profitability compared to pure RO.

We note that the achieved gap between the average and worst case (5th quantile) realized profit is nearly identical (~3%, not shown in table) for both pure RO and BIO 25% and 35%. Thus

the overall results indicates that a calibrated bimodal inventory strategy can considerably boost average gain without compromising on the (practical) worst case performance. This performance gain can be attributed to BIO's ability to value different inventory positions using a 'bifocal' optimistic and pessimistic lens that either improves or preserves the average and (practical) worst case KPIs, while being data-driven and distribution-free.

We recommend the use of the BIO model when it is compatible with the application (e.g., in an omnichannel case) and exercising caution when increasing the value of λ beyond 50% given the potential impact on profitability metrics.

Appendix A: Extension to incorporate the movement of pre-existing inventory across nodes

We show how we extend the main model when in addition to supplier purchase, we consider the movement of pre-existing inventory from different nodes in the network to other nodes (say warehouse to store allocation of fashion items). Here we refer to S as the supplier node and define (1) $C_{l'}$ as the per-unit transportation or purchase when shipping from node or supplier $l' \in \Lambda \cup S$ to node l (and use it instead of C_l); (2) $L_{l'}$ as the lead time between nodes l and l' where L_l is the maximum lead time for node l , in particular, $\max_{l' \in \Lambda \cup S} L_{l'}$, and (3) $x_{tl}^{l'}$ as the inventory allocated from node $l' \in \Lambda \cup S$ in period t for node l .

The model changes as follows. In the objective 4.3, we replace term $C_l x_t^l$ by $\sum_{l' \in \Lambda \cup S} C_{l'} x_{tl}^{l'}$. Next, we replace constraints (4.6) and (4.7) as follows:

$$s_{tl}^b + \sum_{z \in Z} y_{tlz} + I_{t+1,l}^0 = I_{tl}^0 + I_{tl}^1 \mathbb{1}_{L_l > 0} + \sum_{l' \in \Lambda \cup S} x_{tl}^{l'} \mathbb{1}_{L_{l'} = 0} - \sum_{l' \in \Lambda} x_{tl}^{l'} \quad \forall l \in \Lambda, \quad (\text{A.1})$$

$$I_{t+1,l}^j = I_{tl}^{j+1} \mathbb{1}_{j < L_l} + \sum_{l' \in \Lambda \cup S} x_{tl}^{l'} \mathbb{1}_{L_{l'} = j} \quad \forall 1 \leq j \leq L_l, l \in \Lambda \quad (\text{A.2})$$

Also, in the static robust formulation, constraint (4.9) can be rewritten as:

$$s_{tl}^b + \sum_{z \in Z} y_{tlz} + I_{t+1,l} = I_{tl} + \bar{I}_l^{t+1} \mathbb{1}_{t < L_l} + \sum_{l' \in \Lambda \cup S} x_{t-L_{l'},l}^{l'} \mathbb{1}_{t \geq L_{l'}} - \sum_{l' \in \Lambda} x_{tl}^{l'} \quad \forall l \in \Lambda. \quad (\text{A.3})$$

Appendix B: Optimistic-robust modeling to exploit an information edge

There are alternative ways of developing an allied-adversary. For example, we can have λ being time-dependent, channel dependent or even location-dependent. For the uncertainty set we adopt, time or channel dependent λ does not significantly affect our results. On the other hand, a location-specific λ enables us to model use cases where we can allow pure optimism in some locations, say at most Q in number, and

only permit pure adversarial demands in others. The specific optimistic locations (or location clusters) can be configured by the user based on an information ‘edge’, i.e., extraneous demand signals that indicate an increased chance of a sales spike. Note that by tuning a λ parameter by location using a validation dataset, we can obtain an SAA-like approximation within our BIO setting. On the other hand, the challenge with introducing location dependence is that the resultant demand may not longer belong to the uncertainty set we use in our formulation. In an iterative algorithm like CCG, the previously elicited adversarial demands together with the current optimistic demand in the master, are not guaranteed to lie within the set U (even though they were feasible to some of the past realizations of the optimistic demand). An elastic uncertainty set can be introduced to mitigate this limitation, and the resultant BIO approximation can be practically useful in its ability to exploit an information edge.

Appendix C: Closed form solutions for a single location walk-in setting

PROPOSITION 3. For a single location problem with time-horizon $T = 1$ and zero lead time, if the uncertainty set $U = [D_{\min}, D_{\max}]$ and initial inventory $I^0 = 0$, the optimal pure robust and best case solutions and their respective objective functions are obtained as follows assuming $p + b \geq c > 0$:

$$x_{BIO-1}^* = \begin{cases} D_{\max} & \text{if } p \geq c \\ 0 & \text{otherwise.} \end{cases}, \quad Z_{BIO-1}^* = \begin{cases} (p-c)D_{\max} & \text{if } p \geq c \\ (p-c)D_{\min} & \text{otherwise.} \end{cases} \quad (C.1)$$

$$x_{BIO-0}^* = \frac{(p+h)D_{\min} + bD_{\max}}{(p+b+h)}, \quad Z_{BIO-0}^* = \frac{(p+b-c)(p+h)D_{\min} - (h+c)bD_{\max}}{(p+b+h)} \quad (C.2)$$

With proposition 1, we can obtain $x_{BIO-\lambda}^*$ and $Z_{BIO-\lambda}^*$ in closed form. Also, we know that the closed form newsvendor solution in this case is $x_{SAA}^* = VaR_D\left(\frac{p+b-c}{p+b+h}\right)$

Proof: Let us understand the best case and worst demand in a simple setting of a single location and single time period. Now let us consider the pure robust setting.

$$\begin{aligned} & \max_x \min_{D_{\min} \leq D \leq D_{\max}} (p-c)D - (p+b-c)(D-x)^+ - (h+c)(x-D)^+ \\ \implies & \max_x \begin{cases} (p+h)D_{\min} - (h+c)x & \text{if } x \geq \frac{(p+h)D_{\min} + bD_{\max}}{(p+b+h)} \\ (p+b-c)x - bD_{\max} & \text{otherwise} \end{cases} \\ \implies & x^* = \frac{(p+h)D_{\min} + bD_{\max}}{(p+b+h)} \text{ if } p+b \geq c \text{ and Opt Obj} = \frac{(p+b-c)(p+h)D_{\min} - (h+c)bD_{\max}}{(p+b+h)} \end{aligned}$$

Now let us study the best case problem:

$$\max_x \max_{D_{\min} \leq D \leq D_{\max}} (p-c)D - (p+b-c)(D-x)^+ - (h+c)(x-D)^+$$

$$\implies \max_x (p-c)x \quad \text{where } D_{\min} \leq x \leq D_{\max}$$

$$\implies x^* = D_{\max} \text{ if } p \geq c, \text{ else } 0.$$

□

Appendix D: Proof of Theorem 1

THEOREM 1. *Given λ , there exists an $x_{BIO-\lambda}^*$ such that $x_{BIO-\lambda}^* = \lambda x_{BIO-1}^* + (1-\lambda)x_{BIO-0}^*$ and the corresponding optimal objective value $Z_{BIO-\lambda}^*$ satisfies $Z_{BIO-\lambda}^* = \lambda Z_{BIO-1}^* + (1-\lambda)Z_{BIO-0}^*$. In other words, for any given λ , there exists an optimal allocation for $BIO-\lambda$ that is a linear superposition of the respective optimal quantities for the best case scenario (when $\lambda = 1$, i.e., $BIO-1$) and the robust scenario (when $\lambda = 0$, i.e., $BIO-0$). Moreover, the optimal objective value follows the same superposition structure.*

Proof: The above result holds when λ equals 0 or 1 immediately. So, we will now consider a case when $0 < \lambda < 1$. Let us refer to the $BIO-\lambda$ problem as $P^{BIO-\lambda}$. We first show bi-directional feasibility, that is: (1) any feasible solution of the problems P^{BIO-0} and P^{BIO-1} , can be combined to arrive at a feasible solution for $P^{BIO-\lambda}$ and (2) any feasible solution to $P^{BIO-\lambda}$ can be disaggregated to arrive at feasible solutions to P^{BIO-0} and P^{BIO-1} .

We use the following notation for feasible solutions for $P^{BIO-\lambda}$, P^{BIO-0} and P^{BIO-1} respectively: $\{x, D_\lambda^+, D_\lambda^-, s, y, I\}$, $\{x^+, D^+, s^+, y^+, I^+\}$ and $\{x^-, D^-, s^-, y^-, I^-\}$. If $\{x, D_\lambda^+, D_\lambda^-, s, y, I\}$ is a feasible solution to $P^{BIO-\lambda}$, we know that the following equations are satisfied $\forall t \in \mathcal{T}$:

$$s_{tl}^b \leq \lambda D_{tl}^{b+} + (1-\lambda)D_{tl}^{b-} \quad \forall l \in \Lambda, \quad (\text{D.1})$$

$$\sum_{l \in \Lambda} y_{tlz} \leq \lambda D_{tz}^{o+} + (1-\lambda)D_{tz}^{o-} \quad \forall z \in Z, \quad (\text{D.2})$$

$$s_{tl}^b + \sum_{z \in Z} y_{tlz} + I_{t+1,l} = I_{tl} + \bar{I}_l^{t+1} \mathbb{1}_{t < L_l} + x_{t-L_l,l} \mathbb{1}_{t \geq L_l} \quad \forall l \in \Lambda, \quad (\text{D.3})$$

$$I_{0l} = \bar{I}_l^0 \quad \forall l \in \Lambda. \quad (\text{D.4})$$

If $\{x^+, D^+, s^+, y^+, I^+\}$ and $\{x^-, D^-, s^-, y^-, I^-\}$ are feasible solutions to P^{BIO-0} and P^{BIO-1} respectively, we know that the following equations are satisfied $\forall t \in \mathcal{T}$:

$$s_{tl}^{b+} \leq D_{tl}^{b+}, \quad s_{tl}^{b-} \leq D_{tl}^{b-} \quad \forall l \in \Lambda, \quad (\text{D.5})$$

$$\sum_{l \in \Lambda} y_{tlz}^+ \leq D_{tz}^{o+}, \quad \sum_{l \in \Lambda} y_{tlz}^- \leq D_{tz}^{o-} \quad \forall z \in Z, \quad (\text{D.6})$$

$$s_{tl}^{b+} + \sum_{z \in Z} y_{tlz}^+ + I_{t+1,l}^+ = I_{tl}^+ + \bar{I}_l^{t+1} \mathbb{1}_{t < L_l} + x_{t-L_l,l}^+ \mathbb{1}_{t \geq L_l} \quad \forall l \in \Lambda, \quad (\text{D.7})$$

$$s_{tl}^{b-} + \sum_{z \in Z} y_{tlz}^- + I_{t+1,l}^- = I_{tl}^- + \bar{I}_l^{t+1} \mathbb{1}_{t < L_l} + x_{t-L_l,l}^- \mathbb{1}_{t \geq L_l} \quad \forall l \in \Lambda \quad (\text{D.8})$$

$$I_{0l}^+ = \bar{I}_l^0, \quad I_{0l}^- = \bar{I}_l^0 \quad \forall l \in \Lambda \quad (\text{D.9})$$

It is easy to see that every feasible solution of the problems P^{BIO-0} and P^{BIO-1} can be combined with scaled inventory and fulfillment variables to derive a feasible solution of $P^{BIO-\lambda}$ as follows: $\{x, s, y, I\}_\lambda = \lambda\{x^+, s^+, y^+, I^+\} + (1 - \lambda)\{x^-, s^-, y^-, I^-\}$, $\{D^+\}_\lambda = \{D^+\}$ and $\{D^-\}_\lambda = \{D^-\}$ where all operations are element-wise. And because the fulfillment and inventory variables are scaled, along with the demand, the resultant objective is a superposition of the two objectives³, i.e., $Z_{BIO-\lambda} = \lambda Z_{BIO-1} + (1 - \lambda) Z_{BIO-0}$, where the objectives correspond to the feasible solutions being considered.

We will now show that any feasible solution to the problem $P^{BIO-\lambda}$ can be used to generate a feasible solution to the problems P^{BIO-0} and P^{BIO-1} . Note that the constraints of $P^{BIO-\lambda}$ can be viewed as linear superpositions of the respective constraints of the two problems P^{BIO-0} and P^{BIO-1} , barring the respective upper and lower bounds of the individual variables. So, there may be many feasible solutions to the disaggregated set of constraints and here we show how we generate one of these. We let the demand remain the same across the problems, i.e., $\{D^+\}_{P^{BIO-1}} = \{D^+\}_\lambda$ and $\{D^-\}_{P^{BIO-0}} = \{D^-\}_\lambda$. We first generate sales and fulfillment variables to satisfy the constraints (D.5-D.6) that ensures that the sales are less than the channel-specific demand in every period and location. The sales less than demand constraints are separable by period and so the following discussion regarding fulfillment variables (s, y) is per period and we drop the subscript t for convenience. We begin with the walk-in channel where we can further decompose the constraints by location. we set the sales values as follows: $\{s^+\} = \min\{\{D\}^+, \{s\}/\lambda\}$ and $\{s^-\} = (\{s\} - \lambda\{s^+\})/(1 - \lambda)$. Note that because of the way we set the optimistic sales, the pessimistic portion of the sales also satisfies the sales less than its respective demand constraint (D.5). For the y variables, we first order the location in an enumerated sequence, say $l = 1, 2, \dots, |\Lambda|$ and then $y_{lz}^+ = \min\{\max\{0, D_z^+ - \sum_{l' < l} y_{l'z}^+\}, y_{lz,\lambda}/\lambda\}$ and $y_{lz}^- = (y_{lz,\lambda} - \lambda y_{lz}^+)/ (1 - \lambda)$. Similarly to the walk-in case, these fulfillment values also satisfy the counterpart constraint (D.6).

³ Note that if we used a channel specific λ (as we did in in equations 4.12-4.16), then we use the same channel specific λ for the fulfillment variables here. The proof is indifferent to this choice and works in the general case too.

What remains to be identified are $\{x^+, I^+\}$ and $\{x^-, I^-\}$ for each location $l \in \Lambda$. For simplified notation, we let $S_{il}^+ = s_{il}^{b+} + \sum_{z \in Z} y_{ilz}^+$ and $S_{il}^- = s_{il}^{b-} + \sum_{z \in Z} y_{ilz}^-$. We skip subscript l as the same logic follows for each $l \in \Lambda$. We first identify the optimistic variables $\{x^+, I^+\}$ with S_t^+ as inputs by solving the following LP. Here we choose an arbitrary finite $c > h > 0$ (motivating purchasing as little inventory as needed with minimal holding to meet sales S_t^+):

$$\min_{I^+, x^+ \geq 0} \sum_{t=0}^T [hI_{t+1}^+ + c\hat{x}_t^+] \quad (\text{D.10})$$

$$S_t^+ + I_{t+1}^+ = I_t^+ + \bar{I}^{t+1} \mathbb{1}_{t < L} + x_{t-L}^+ \mathbb{1}_{t \geq L} \quad \forall t \in \{0, \dots, T-1\} \quad (\text{D.11})$$

$$\lambda x_t^+ \leq x_t \quad \forall t \in \{0, \dots, T-1\} \quad (\text{D.12})$$

$$I_0^+ = \bar{I}^0 \quad (\text{D.13})$$

We know this is feasible as $P^{BIO-\lambda}$ was feasible and because $\lambda S_t^+ \leq S_t$ per our earlier selection. We then set $\{I^-\} = (\{I\}_\lambda - \lambda\{I^+\})/(1-\lambda)$ and $\{\hat{x}^-\} = (\{\hat{x}\}_\lambda - \lambda\{\hat{x}^+\})/(1-\lambda)$. Observe that by design $\{\hat{x}^+, I^+\}$ and $\{\hat{x}^-, I^-\}$ are non-negative and $\{\hat{x}^-, S^-, I^-\}$ satisfy the inventory balance constraints of P^{BIO-0} . This can be gathered by eliminating the terms related to $\{\hat{x}^+, S^+, I^+\}$ in $P^{BIO-\lambda}$. Moreover, because the λ -superposition of each feasible variable is maintained, the $BIO-0, BIO-1$ objectives also satisfy the λ -superposition, i.e., $Z_{BIO-\lambda} = \lambda Z_{BIO-1} + (1-\lambda)Z_{BIO-0}$.

Now having shown bi-directional feasibility, we begin with the optimal solution to problem $P^{BIO-\lambda}$. We then generate feasible solutions to problems P^{BIO-0} and P^{BIO-1} . Each of these can be improved to its respective optimal solution which is again feasible to $P^{BIO-\lambda}$ which by definition cannot have a better objective than the optimal solution we began with. This means each step here resulted in an optimal transition and therefore there exists an optimal allocation x to $P^{BIO-\lambda}$, i.e., $x_{BIO-\lambda}^*$ such that $x_{BIO-\lambda}^* = \lambda x_{BIO-1}^* + (1-\lambda)x_{BIO-0}^*$ and it corresponds to an optimal objective $Z_{BIO-\lambda}^*$ that satisfies $Z_{BIO-\lambda}^* = \lambda Z_{BIO-1}^* + (1-\lambda)Z_{BIO-0}^*$. Hence, the theorem. \square

Appendix E: Proof of Proposition 1

PROPOSITION 4. *The extreme points of the uncertainty set U described in Eq.(3.1) with integral bounds are integral.*

Proof: Because the set U in Eq.(3.1) decomposes by channel and time period, without loss of generality we only present the result for the walk-in channel and for a single time period by dropping the time subscript. To prove integrality, we consider the following LP where $c_l \forall l \in \Lambda$ can be chosen to be any vector of constants:

$$\min_{D_l} \sum_{l \in \Lambda} c_l D_l \quad (\text{E.1})$$

$$\bar{D}_l^L \leq D_l \leq \bar{D}_l^U \quad \forall l \in \Lambda \quad (\text{E.2})$$

$$\bar{D}^L \leq \sum_{l \in \Lambda} D_l \leq \bar{D}^U \quad (\text{E.3})$$

Consider any corresponding optimal solution of this LP. We want to show that there exists an extreme point solution to the LP that is integral and optimal assuming $\bar{D}_l^L, \bar{D}_l^U \forall l \in \Lambda$ and \bar{D}^L, \bar{D}^U are integral.

Case 1: If all but one location say l' have integral D_l then $D_{l'}$ can also be chosen to be integral by decreasing or increasing to the nearest integer depending on whether $c_{l'} \leq 0$ or vice versa, and without loss of generality, this move will only improve the optimal objective.

Case 2: Next, suppose there exists at least one pair of locations that have non-integral solutions. Here, we can decrease the demand for the one with lower c_l and increase the demand in the other location with higher c_l (if the costs are equal, then pick any one location arbitrarily) until one of demand variables hits a local lower or upper bound without impacting the budget constraint. At this point we have decreased the number of locations with non-integral demands by 1 and improved the objective, if at all. If we repeat this procedure for every pair of non-integral demand locations, we will reduce the problem to the case of non-integrality at no more than one location, which can be resolved per Case-1 discussed earlier. \square

Appendix F: Proof of Proposition 2

Proof: Constraints (5.10-5.12) together with the binary nature of w describe the discrete elements of the uncertainty set U . We know this is a just a sub-set of U but contains the optimal adversarial demand solution to the problem due to Proposition 1. Note that we are implicitly enforcing the following superposition constraints in the budget restrictions (5.11-5.12) : $D_{tl}^b = \sum_{k \in K_{tl}^b} \bar{D}_{tlk}^b w_{tlk}^b$; $D_{tz}^o = \sum_{k \in K_{tz}^o} \bar{D}_{tzk}^o w_{tzk}^o$. We linearize the bilinear terms in the objective by setting $\alpha_{tlk}^* = \alpha_{tl} w_{tlk}^b$ and $\beta_{tlk}^* = \beta_{tl} w_{tlk}^o$ and employ the relaxation and linearization technique (RLT) to exactly linearize these terms utilizing the binary nature of variables w and the definition of M to get constraints (5.8-5.9). \square

Note that M can be tightened by having it tailored by time period and node or zone in an actual implementation, more specifically with $M_{tl} = p_{tl}^b + b_{tl}^b + (T-t)h_l$, $M_{tz} = p_t^o + b_t^o + \max_{l \in \Lambda} \{(T-t)h_l - c_{lz}\}$.

Appendix G: Adaptation of the CCG method to solve BIO- λ problem

We incorporate the exact MIP sub-problem given in Proposition 2 within the column and cut generation (CCG) framework proposed by Zeng and Zhao (2013) to solve two-stage linear optimization problems. An important aspect of our sub-problem is that its feasibility is guaranteed regardless of the values of its inputs $(\mathbf{x}, \mathbf{s}^{b+})$, i.e., the solution space is non-empty, because zero fulfillment is always a feasible solution. This means we satisfy the *relatively complete recourse* assumption. This holds even in the presence of additional business rules such as fulfillment capacity constraints or fulfillment time-window goals, as a zero fulfillment is readily available as a feasible solution. The CCG framework by Zeng and Zhao (2013) only address problems that satisfies this property, which suffices for our setting. For generalizations, refer to Bertsimas and Shtern (2018)'s extension of the CCG framework.

In the CCG method, a master problem is formulated using a finite set of feasible \mathbf{D}^- uncertainty values. Let $\{\mathbf{D}^1, \dots, \mathbf{D}^j\}$ a set of feasible demand vectors for $\mathbf{D}^- \in U$. We formulate the master problem as follows which we denote by $MP_j = MP(\{\mathbf{D}^1, \dots, \mathbf{D}^j\})$:

$$Z^{MP_j} = \max_{\substack{\eta, \mathbf{D}^+ \in U \\ (x, s^+, s^-, y, I) \geq 0}} \eta + \sum_{t \in \mathcal{T}} \sum_{l \in \Lambda} [(p_{tl}^b + b_{tl}^b) s_{tl}^{b+} - b_{tl}^b \lambda D_{tl}^{b+} - C_l x_{tl}] \quad (\text{G.1})$$

subject to

$$\eta \leq \sum_{t \in \mathcal{T}, l \in \Lambda} \left[(p_{tl}^b + b_{tl}^b) s_{tl}^{bi-} + \sum_{z \in \mathcal{Z}} (p_t^o + b_t^o - c_{tz}) y_{tlz}^i - b_{tl}^b (1 - \lambda) D_{tl}^{bi-} - h_l I_{t+1,l}^i \right] - \sum_{t \in \mathcal{T}, z \in \mathcal{Z}} b_t^o D_{tz}^{oi} \quad \forall i < j \quad (\text{G.2})$$

$$s_{tl}^{b+} \leq \lambda D_{tl}^{b+} \quad \forall l \in \Lambda, t \in \mathcal{T} \quad (\text{G.3})$$

$$s_{tl}^{bi-} \leq (1 - \lambda) D_{tl}^{bi-} \quad \forall l \in \Lambda, t \in \mathcal{T}, i < j \quad (\text{G.4})$$

$$\sum_{l \in \Lambda} y_{tlz}^i \leq D_{tz}^{oi} \quad \forall z \in \mathcal{Z}, t \in \mathcal{T}, i < j \quad (\text{G.5})$$

$$s_{tl}^{b+} + s_{tl}^{bi-} + \sum_{z \in \mathcal{Z}} y_{tlz}^i + I_{t+1,l}^i = I_{tl}^i + \bar{I}_l^{t+1} \mathbb{1}_{t < L_l} + x_{t-L_l,l} \mathbb{1}_{t \geq L_l} \quad \forall l \in \Lambda, t \in \mathcal{T}, i < j \quad (\text{G.6})$$

$$I_{0l}^i = \bar{I}_{0l}^0 \quad \forall l \in \Lambda, i < j \quad (\text{G.7})$$

The CCG algorithm given below solves the master and the sub-problem alternatively until the desired tolerance-based stopping criterion is satisfied. This solution technique can be viewed as the master program generating a sequence of beneficial allocations, the sub-problem adding corresponding adversarial demand ‘cuts’ to master and the iterations stop when the master problem converges in their achieved objective.

Algorithm 1 Column and Cut Generation (CCG) Approach to inventory allocation**Input:** Stopping criteria tolerance ϵ and a small number δ (say 10^{-5})**Initialize:** $j = 0$, $LB^0 = -\infty$, $UB^0 = +\infty$, demand sample set $U^0 = \{\mathbf{D}^0\}$, $\mathbf{x}^* = \mathbf{0}$

1. $j := j+1$
2. Solve master problem $MP(U^j)$ to get $(\mathbf{x}^j, \mathbf{s}^{b+,j}, \eta^j)$ and update $UB^j = Z^{MP_j}$.
3. Solve sub-problem $SP(\mathbf{x}^j, \mathbf{s}^{b+,j})$ to get \mathbf{D}^j and update $LB^j = \max\{LB^{j-1}, Z^{SP(\mathbf{x}^j, \mathbf{s}^{b+,j})} + Z^{MP_j} - \eta^j\}$ and $U^j = U^{j-1} \cup \{\mathbf{D}^j\}$. Also, if $LB^j = Z^{SP(\mathbf{x}^j, \mathbf{s}^{b+,j})} + Z^{MP_j} - \eta^j$, update $\mathbf{x}^* = \mathbf{x}^j$
4. If $\frac{UB^j - LB^j}{|LB^j| + \delta} \leq \epsilon$, return \mathbf{x}^* . Otherwise go to step 1.

PROPOSITION 5. (Zeng and Zhao 2013) Algorithm 1 converges to an optimal solution of SBIO- λ problem in finite iterations.

Note that the CCG method and its finite convergence to optimality is independent of the type of continuous or integral set chosen for the allocations x and D^+ . It assumes that an oracle is used to solve the sub-problem to optimality (or alternatively each time a new extreme point or discrete demand is elicited and incorporated).

Note also that we return the allocation \mathbf{x}^* , defined as the allocation that yields the best lower-bound computed this far, instead of \mathbf{x}^j , the current master problem solution. The intuition is that the sub-problem objective captures the true value of an allocation and that might not increase through the iterations as the algorithm explores various first stage solutions. We include a pictorial representation of this intuition in Fig. 6. With this modification and other practical safeguards one may impose such as tolerance or time limits, we end up finding the best solution with the available resources, and noting that more iterations/time leads to improvement in solution quality.

References

- Acimovic J, Graves SC (2015) Making better fulfillment decisions on the fly in an online retail environment. *Manufacturing & Service Operations Management* 17(1):34–51.
- Acimovic J, Graves SC (2017) Mitigating spillover in online retailing via replenishment. *Manufacturing & Service Operations Management* 19(3):419–436.

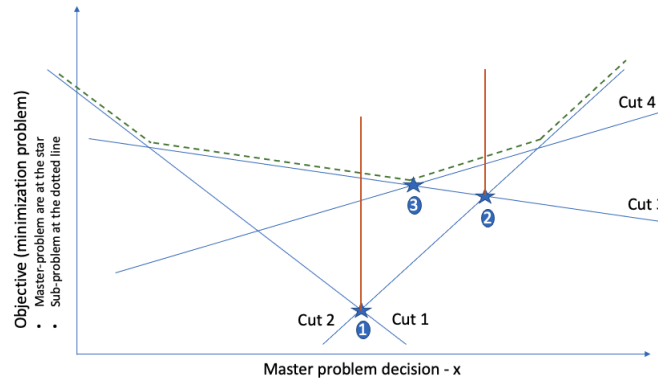


Figure 6 The intuition of how a cut-generation algorithm would proceed for a minimization problem. Observe how the master problem objective serves as a lower bound and the sub-problem objective as an upper bound. Also, observe that at the end of iteration 2, the best solution x is that of iteration 1 as the sub-problem objective is better.

Ali K, Michael D, Ajay D, Arun H, Yingjie L, Xuan L, Christopher M, Brian QL, Raymond T, Yada Z (2017) An optimization framework for a multi-objective omni-channel order fulfilment problem. *IIE Annual Conference. Proceedings*, 2051–2056 (Institute of Industrial and Systems Engineers (IISE)).

Bandi C, Bertsimas D (2012) Tractable stochastic analysis in high dimensions via robust optimization. *Mathematical programming* 134(1):23–70.

Bandi C, Han E, Nohadani O (2019) Sustainable inventory with robust periodic-affine policies and application to medical supply chains. *Management Science* 65(10):4636–4655.

Ben-Tal A, Goryashko A, Guslitzer E, Nemirovski A (2004) Adjustable robust solutions of uncertain linear programs. *Mathematical programming* 99(2):351–376.

Bertsimas D, Brown DB, Caramanis C (2011) Theory and applications of robust optimization. *SIAM review* 53(3):464–501.

Bertsimas D, Gupta V, Kallus N (2018) Robust sample average approximation. *Mathematical Programming* 171:217–282.

Bertsimas D, Shtern S (2018) A scalable algorithm for two-stage adaptive linear optimization. *arXiv preprint arXiv:1807.02812* .

Bertsimas D, Sim M (2004) The price of robustness. *Operations research* 52(1):35–53.

-
- Bourlier A (2020) *Retail Dive* URL <https://www.retaildive.com/news/how-covid-19-prompted-new-thinking-for-omnichannel/592010/>.
- DeValve L, Wei Y, Wu D, Yuan R (2023) Understanding the value of fulfillment flexibility in an online retailing environment. *Manufacturing & service operations management* 25(2):391–408.
- Gallino S, Moreno A (2014) Integration of online and offline channels in retail: The impact of sharing reliable inventory availability information. *Management Science* 60(6):1434–1451.
- Gallino S, Moreno A, Stamatopoulos I (2017) Channel integration, sales dispersion, and inventory management. *Management Science* 63(9):2813–2831.
- Gao F, Su X (2017a) Omnichannel retail operations with buy-online-and-pick-up-in-store. *Management Science* 63(8):2478–2492.
- Gao F, Su X (2017b) Online and offline information for omnichannel retailing. *Manufacturing & Service Operations Management* 19(1):84–98.
- Gorissen BL, Yanıkoğlu İ, den Hertog D (2015) A practical guide to robust optimization. *Omega* 53:124–137.
- Gotoh Jy, Kim MJ, Lim AE (2023) A data-driven approach to beating SAA out-of-sample. *Operations Research* .
- Govindarajan A, Sinha A, Uichanco J (2021a) Distribution-free inventory risk pooling in a multilocation newsvendor. *Management Science* 67(4):2272–2291.
- Govindarajan A, Sinha A, Uichanco J (2021b) Joint inventory and fulfillment decisions for omnichannel retail networks. *Naval Research Logistics (NRL)* 68(6):779–794.
- Harsha P, Subramanian S, Ettl M (2019a) A practical price optimization approach for omnichannel retailing. *INFORMS Journal on Optimization* 1(3):241–264.
- Harsha P, Subramanian S, Uichanco J (2019b) Dynamic pricing of omnichannel inventories. *Manufacturing & Service Operations Management* 21(1):47–65.
- Iancu DA, Trichakis N (2014) Pareto efficiency in robust optimization. *Management Science* 60(1):130–147.
- Jackson PL, Muckstadt JA, Li Y (2019) Multiperiod stock allocation via robust optimization. *Management Science* 65(2):794–818.

- Jasin S, Sinha A (2015) An lp-based correlated rounding scheme for multi-item ecommerce order fulfillment. *Operations Research* 63(6):1336–1351.
- Jati A, Ekambaram V, Pal S, Quanz B, Gifford WM, Harsha P, Siegel S, Mukherjee S, Narayanaswami C (2023) Hierarchical proxy modeling for improved HPO in time series forecasting. *Proceedings of the 29th ACM SIGKDD Conference on Knowledge Discovery and Data Mining*, 891–900, KDD '23.
- Kelly JL (1956) A new interpretation of information rate. *The Bell System Technical Journal* 35(4):917–926.
- Kleywegt AJ, Shapiro A, Homem-de Mello T (2002) The sample average approximation method for stochastic discrete optimization. *SIAM Journal on optimization* 12(2):479–502.
- Lei Y, Jasin S, Sinha A (2018) Joint dynamic pricing and order fulfillment for e-commerce retailers. *Manufacturing & Service Operations Management* 20(2):269–284.
- Lim YF, Jiu S, Ang M (2021) Integrating anticipative replenishment allocation with reactive fulfillment for online retailing using robust optimization. *Manufacturing & Service Operations Management* 23(6):1616–1633.
- Lim YF, Wang C (2017) Inventory management based on target-oriented robust optimization. *Management Science* 63(12):4409–4427.
- Makridakis S, Spiliotis E, Assimakopoulos V (2022) M5 accuracy competition: Results, findings, and conclusions. *International Journal of Forecasting* 38(4):1346–1364, ISSN 0169-2070, URL <http://dx.doi.org/https://doi.org/10.1016/j.ijforecast.2021.11.013>, special Issue: M5 competition.
- Nageswaran L, Cho SH, Scheller-Wolf A (2020) Consumer return policies in omnichannel operations. *Management Science* 66(12):5558–5575.
- NeilsonIQ (2022) URL <https://nielseniq.com/global/en/insights/success-story/2022/pivoting-to-long-term-growth-with-omnichannel-strategy/>.
- Oreshkin BN, Carpov D, Chapados N, Bengio Y (2020) N-beats: Neural basis expansion analysis for interpretable time series forecasting. *International Conference on Learning Representations*.
- Paterson C, Kiesmüller G, Teunter R, Glazebrook K (2011) Inventory models with lateral transshipments: A review. *European Journal of Operational Research* 210(2):125–136.

-
- Rahimian H, Mehrotra S (2019) Distributionally robust optimization: A review. *arXiv preprint arXiv:1908.05659* .
- Rotando LM, Thorp EO (1992) The Kelly criterion and the stock market. *The American Mathematical Monthly* 99(10):922–931.
- Salinas D, Flunkert V, Gasthaus J (2019) DeepAR: Probabilistic forecasting with autoregressive recurrent networks. *International Journal of Forecasting* 8(2):136–153.
- Saénz MJ, Revilla E, Borrella I (2022) Digital transformation is changing supply chain relationships. *Harvard Business Review* .
- Sherali HD, Adams WP (1998) Reformulation-linearization techniques for discrete optimization problems. *Handbook of Combinatorial Optimization: Volume1–3* 479–532.
- Simchi-Levi D, Wang H, Wei Y (2019) Constraint generation for two-stage robust network flow problems. *INFORMS Journal on Optimization* 1(1):49–70.
- Tagaras G, Cohen MA (1992) Pooling in two-location inventory systems with non-negligible replenishment lead times. *Management science* 38(8):1067–1083.
- Xin L (2021) Understanding the performance of capped base-stock policies in lost-sales inventory models. *Operations Research* 69(1):61–70.
- Yang J, Qin Z (2007) Capacitated production control with virtual lateral transshipments. *Operations research* 55(6):1104–1119.
- Zeng B, Zhao L (2013) Solving two-stage robust optimization problems using a column-and-constraint generation method. *Operations Research Letters* 41(5):457–461.